Latitudinal distribution of biomarkers across the western Arctic Ocean and the Bering Sea: an approach to assess sympagic and pelagic algal production

5 Youcheng Bai[1,2], Marie-Alexandrine Sicre[3], Jian Ren[1,2], Vincent Klein[3], Haiyan Jin[1,2,4] and Jianfang Chen[1,2,5*]

[1]Key Laboratory of Marine Ecosystem Dynamics, Ministry of Natural Resources, Hangzhou 310012, China

10 [2]Second Institute of Oceanography, Ministry of Natural Resources, Hangzhou 310012, China

[3]LOCEAN, CNRS, Sorbonne Université, Campus Pierre et Marie Curie, Case 100, 4 Place Jussieu, 75032, Paris, France

[4]School of Oceanography, Shanghai Jiao Tong University, Shanghai 200230, China

[5]State Key Laboratory of Satellite Ocean Environment Dynamics, Second Institute of

15 Oceanography, Ministry of Natural Resources, Hangzhou 310012, China

Corresponding to: Jianfang Chen (jfchen@sio.org.cn)

Abstract. The drastic decline of Arctic sea ice due to global warming and polar amplification of environmental changes in the Arctic basin profoundly alter primary production with

20   consequences for polar ecosystems and the carbon cycle. In this study, we use highly branched isoprenoids (HBIs), brassicasterol, dinosterol and terrestrial biomarkers (*n*-alkanes and campesterol) in surface sediments to assess sympagic and pelagic algal production with changing sea-ice conditions along a latitudinal transect from the Bering Sea to the high latitudes of the western Arctic Ocean. Suspended particulate matter (SPM) was also collected in surface

25   waters at several stations of the Chukchi Sea to provide snapshots of phytoplankton communities under various sea-ice conditions for comparison with underlying surface sediments. Our results show that sympagic production (IP_{25} and HBI-II) increased northward between 62°N and 73°N, with maximum values at the sea-ice edge in the Marginal Ice Zone (MIZ) between 70°N and 73°N in southeastern Chukchi Sea and along the coast of Alaska.

30   They were consistently low at northern high latitudes (>73°N) under extensive summer sea-ice cover and in the Ice-Free Zone (IFZ) of the Bering Sea. Enhanced pelagic sterols and HBI-III occurred in the IFZ across the Bering Sea and in southeastern Chukchi Sea up to 70°N-73°N in the MIZ conditions that marks a shift of sympagic over pelagic production. In surface water SPM, pelagic sterols display similar patterns as Chl *a,* increasing southwards with higher

35   amounts found in the Chukchi shelf pointing out the dominance of diatom production. Higher cholesterol values were found in the mid-Chukchi Sea shelf where phytosterols were also abundant. This compound prevailed over phytosterols in sediments, compared to SPM, reflecting efficient consumption of algal material in the water column by herbivorous zooplankton.

1. Introduction

The Arctic Ocean is undergoing the most rapid climate and environmental changes of the world ocean with notably the drastic reduction of sea-ice cover and thickness and increased freshwater from higher Arctic river flows (IPCC, 2021). This rapid sea-ice retreat due to global warming has major consequences not only on sea-ice ecosystems thriving in and below sea ice and their diversity, but also on pelagic phytoplankton and zooplankton communities and subsequently on the food chain (Ardyna et al., 2014; Ardyna and Arrigo, 2020). Surface freshening caused by sea-ice melting and higher river run-off induce changes of phytoplanktonic species (Park et al., 2023) thereby altering the composition, export and sequestration of organic carbon in marine sediments and ultimately the Arctic marine carbon sink (Brown et al., 2020; Coupel et al., 2015; Su et al, 2023). In general, at the onset of the spring bloom beginning period (April-July), diatoms and large phytoplankton are dominant, while the percentage of smaller phytoplankton increases in later summer/early autumn, and thus organic carbon fluxes to the sediments are mainly driven by larger phytoplankton cells (Moran et al., 2012). Li et al. (2009) evidenced a shift towards smallest phytoplankton cells at the expense of larger cells as a result of upper water column stratification. While smaller size picoplankton is efficient in using nutrients and light under stratified conditions, it is less prone to sinking due to low cell density and thus does not support large vertical export as opposed to micro phytoplankton such as diatoms (Li et al., 2009). Such shifts in the quantity and phytoplankton communities need to be better assessed to understand production pathways and impact on secondary production, including microbial communities, and higher trophic levels as well as export and sequestration of organic carbon to the deep ocean, known as the biological pump (Lannuzel et al., 2020).

Sea ice provides a habitat for a wide array of microalgae, bacteria, autotrophic, mixotrophic and heterotrophic protists (Gradinger, 1999; Hop et al., 2020). Ice-associated production (sympagic) is higher in the bottom of the sea ice due to the nutrient supply from the underlying seawater (Arrigo, 2017; Brown et al., 2011). Ice algae are also an important component in the transfer of organic carbon to deeper layers because they form aggregates that can sink faster (Boetius et al., 2013). Usually, they sink very fast as episodic events similar to sea-ice melting. Estimates of the contribution of sympagic to primary production varies from 0 to 80% depending on the sea-ice type, region and season and are thus difficult to assess basin-wide (Ehrlich et al., 2021; Gosselin et al., 1997; Legendre et al., 1992). Boetius et al. (2013) reported that in summer 2012 of unprecedented decline of sea ice, macro-aggregates of diatom *Melosira arctica* contributed at least 45% of total primary productivity and more than 85% of carbon export in the central Arctic basin between 82°N and 89°N. The increased area of thin seasonal sea ice and melt ponds with sea ice due to global warming is likely to affect phytoplankton

carbon uptake and export. The longer season for primary production due to earlier melting and later freezing is another parameter that will likely enhance carbon uptake in the future.

Organic biomarkers can be used to evaluate sympagic and pelagic primary production. Among them, the mono-unsaturated highly branched isoprenoid alkene (HBI), known as IP_{25} (Ice Proxy with 25 carbon atoms), is a well-established biomarker of sea-ice diatoms of the genera *Haslea and Pleurosigma* (Belt et al., 2007; Brown et al., 2014a). The diene, HBI-II, is biosynthesised as well by sympagic diatoms and generally present with IP_{25} in northern polar oceans (Belt and Müller, 2013). In contrast, the triene, HBI-III, is believed to be produced by pelagic diatoms and has subsequently been proposed as an indicator of pelagic algal production (Belt et al., 2017), partly owing to its occurrence in sediments at the sea-ice edge or under ice-free conditions in summer (Belt et al., 2015; Schmidt et al., 2018; Smik et al., 2016).

IP_{25} was initially proposed by Belt et al. (2007) as a proxy of seasonal sea ice. Since the first high-resolution reconstruction published by Massé et al. (2008) in the Nordic Seas, HBIs have been extensively used in paleoceanographic studies to achieve semi-quantitative estimates of seasonal sea-ice extent (Belt, 2018 and reference therein; Kolling et al., 2020, 2023; Müller et al., 2011; Stein et al., 2016). However, few HBI studies have been conducted to assess sympagic versus pelagic production in the western Arctic Ocean and Bering Sea (Koch et al., 2020a, b). In this study, HBIs were used together with selected phyto-sterols to explore the relationship between sympagic-pelagic algal production and sea-ice conditions across a latitudinal transect in the Bering and Chukchi Sea under rapidly sea-ice decline. For this purpose, we also used earlier data from Bai et al. (2019), focussed on PIP_{25} assessment, to get a more complete picture of changing primary production between 54.6 °N and 85.4 °N. Suspended particles were also collected in surface waters in summer 2014 at 13 stations for sterol analyses and compared with surface sediments to insight export pathways.

2. Regional settings

The two main surface ocean currents of the Bering Sea basin are the eastward Aleutian North Slope Current (ANSC) flowing along the Aleutian Islands (Stabeno and Reed, 1994) and the Bering Slope Current (BSC) flowing along the Bering Sea Slope, originating from the inflow of Alaskan Stream (AS) and driving a large-scale cyclonic circulation in the Bering Sea (Fig. 1). The main hydrological features of the Bering Sea northern shelf include the Anadyr Water (AW) originating from the BSC and the Alaska Coastal Water (ACW) while the surface hydrology of the Chukchi Sea is strongly influenced by the warm northward flowing Pacific Water (PW) entering the Arctic Ocean through the Bering Strait and the seasonal cover of sea ice both playing an important role in the ecology and community composition. The PW has an annual mean transport rate of 0.8 Sv (Roach et al., 1995; Woodgate et al., 2005) and comprises

three water masses (Coachman et al., 1975): i) the colder, saline (> 32.5) and nutrient-rich AW (Grebmeier et al., 1988; Weingartner et al., 2005) in the western side of the northern Bering and Chukchi Sea; ii) the relative warm, low-salinity(< 31.8) and nutrient-depleted ACW (Hunt et al., 2013;Woodgate and Aagaard, 2005) in the eastern side and in between the Bering Shelf Water (BSW) with moderate salinity (31.8-32.5; Woodgate et al., 2005) and nutrient levels, iii) the seasonal southward-flowing Siberian Coastal Current (SCC) in the western Chukchi Sea that usually deflects small amounts of cold fresh waters (~0.1Sv) into the central Chukchi Sea (Weingartner et al., 1999) (Fig. 1).

The northern Bering-Chukchi Sea is one of the largest marginal seas in the Arctic Ocean (Jakobsson et al., 2014) and one of the most productive areas (Arrigo and van Dijken, 2011; Hill et al., 2018). Because of continued nutrients supply from the PW, surface waters in this region maintain a high primary production both during the sea-ice melting season and ice-free waters in summer. With the retreat of sea ice, the algal production associated with sea ice (Gradinger, 2009) as well as the under-ice phytoplankton blooms (Ardyna et al., 2020; Arrigo et al., 2012; Coupel et al., 2012, 2015) provide food to higher trophic levels (Cautain et al., 2022; Ji et al., 2012; Kohlbach et al., 2016; Tedesco et al., 2019). With the thinning and retreat of sea ice triggered by global warming, production and export of carbon from sea-ice algal in the Arctic Ocean will also become increasingly important (Ardyna and Arrigo, 2020). However, the exact implications of the drastic sea-ice reduction of the last decades on marine ecosystems are difficult to predict because of adverse effects on phytoplankton (Harada et al., 2016; Shimada et al., 2006).

3. Material and methods

3.1 Surface sediment sampling

Surface sediment samples were recovered from the western Arctic Ocean, including the Bering Sea, the Bering-Chukchi Shelf and the High Arctic Ocean. 52 surface sediment samples (blue dots in Fig. 1) were collected on the RV *Xuelong* during CHINARE cruises ARC3, ARC4, ARC5 and ARC6 in 2008, 2010, 2012 and 2014, respectively and analysed for biomarkers. In addition, 36 samples obtained during the CHINARE cruises between 2008 and 2014 mostly located in the Chukchi Sea published by Bai et al. (2019) (red dots in Fig. 1) were also used in this study. The total sample set of 88 surface sediments encompasses a latitudinal range from 54.6°N to 85.4°N. Details of sampling locations are provided in Table S1. All surface sediment sampling was carried out using a box-corer. After the box-corer was retrieved, the uppermost 0-2 cm of sediment were sliced on board then placed in a plastic bag and stored at -20°C until further processing.
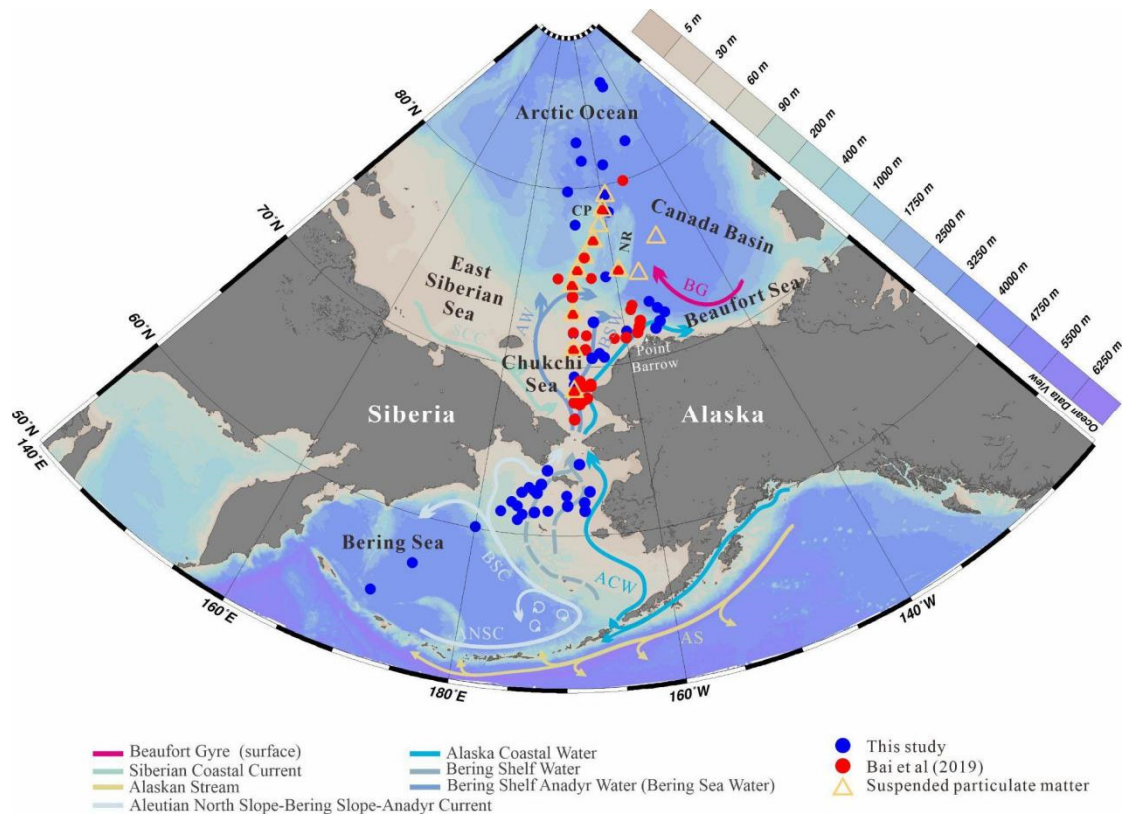
Figure 1. Map showing the location of the 88 surface samples in the Bering Sea and western Arctic Ocean, which includes the new data generated in this study (blue dots) and those earlier published by Bai et al. (2019) (red dots). Orange triangles indicate the sites where surface suspended particulate matter was collected (this study). Arrows feature oceanic surface currents (after Grebmeier et al., 2006). AS-Alaskan Stream; ACW-Alaska Coastal Water; ANSC-Aleutian North Slope Current; BSC-Bering Slope Current; SCC-Siberian Coastal Current; AW-Anadyr Water; BSW-Bering Shelf Water; BG-Beaufort Gyre; CP-Chukchi Plateau; NR-Northwind Ridge. The study area covered the Bering Sea, Chukchi shelf (water depths <140m) and the slope and basin of the western Arctic Ocean (water depths >140m).

3.2 Suspended particles sampling

Suspended particulate matter (SPM) was obtained from the filtration of surface seawater at depths ranging from 0 to 5 m during the summer cruise of the RV *Xuelong* in 2014. A Large Volume Water Transfer System (WTS-LV, Mclane) was used to perform *in situ* filtration of seawater (40-60 L) using glass fibre filters (Whatman GF/F, 142 mm diameter) pre-combusted at 450°C for 4h. After filtration, the particulate-laden filters were stored at -20°C until biomarker analysis. The 13 stations occupied in the Chukchi shelf and Canada basin in summer 2014 (29 July-14 August) are shown in Fig. 1 (orange triangles).

Water samples were also collected for chlorophyll *a* (Chl *a*) analysis using 1 L Niskin bottles during the same summer 2014 cruise on the RV *Xuelong*. Surface water (0.5-1 L) were first filtered through 200 μm Nitex filters to remove zooplankton then sequentially filtered through GF/F filters (Whatman GF/F, 25 mm diameter).

3.3 Total organic carbon (TOC) and Total nitrogen (TN) sediment analyses

Approximately 1g of freeze-dried and homogenized sediment was acidified with 1M hydrochloric acid (HCl) and heated in a water bath at 50°C for at least 48 hours to remove inorganic carbon. Samples were then rinsed with milli-Q grade water until neutral pH was reached (pH=7) and freeze-dried to remove water (Su et al. 2023; Williford et al., 2007). The TOC and TN contents of the surface sediments were measured using an element analyser (FLASH 2000 CHNS-O, Thermo Fisher). BBOT standard of Thermo (carbon% 72.53%; nitrogen% 6.51%) were used for quality control. BBOT standard was measured every 8 samples to correct for drift. The standard deviation of the measurements is less than <0.1%.

3.4 Sample preparation and biomarker extraction

Wet SPM filters and surface sediments were freeze-dried prior to extraction. Lipids were extracted from freeze-dried SPM and from ca. 1-5 g of homogenised sediments using a mixture of dichloromethane/methanol (2:1, v/v). Sediment extraction was performed in a clean glass vial for 10 min in an ultrasonic bath, which was then centrifuged for 2 minutes at 2500 rpm. The supernatant containing the lipids was recovered with a clean glass pipette and transferred in a pre-combusted 8 mL glass vial. This operation was repeated twice and the three extracts combined and dried under a gentle nitrogen stream. For filters, each freeze-dried sample with SPM was cut into small pieces using solvent rinsed scissors and extracted following the same method as for the sediments. Total lipid extracts were then separated into n-alkanes, HBIs and sterols by silica gel chromatography using n-hexane, n-hexane/ethyl acetate (90:10 v/v) and n-hexane/ethyl acetate (70:30 v/v), respectively. About 50 µl BSTFA (bis-trimethylsilyl-trifluoroacetamide) was added to the sterol fractions to convert them into their corresponding trimethylsilyl ethers by heating at 70 °C for 1 hour to complete derivatization before analysis by gas chromatography (GC) on an Agilent Technologies 7890 gas chromatograph coupled to a mass spectrometer (MS) Agilent 262 Technologies 5975C inert XL using a mass selective detector.

3.5 Biomarker analysis

C_{25}-HBIs (IP_{25}, HBI-II, and HBI-III) were analysed by GC/MS. We used a HP-5MS capillary column (30 m long, 0.25 mm i.d., 0.25 µm film thickness) and an oven temperature program from 40 °C to 300 °C at a heating rate of 10 °C/min with a 10 min hold time at final temperature. The operating conditions for the MS were 250 °C for the ion source temperature and 70 eV for the ionisation energy. HBIs were identified by comparing their GC retention times and mass spectra. A known amount of 7-hexylnonadecane (m/z 266) was added as an internal standard

prior extraction for HBI quantification. Selective ion monitoring (SIM) was performed to detect and quantify IP_{25} (*m/z* 350), HBI-II (*m/z* 348) and HBI-III Z isomers (*m/z* 346).

Sterols and *n*-alkanes were analysed by GC using a Varian 3300 equipped with a septum programmable injector (SPI) and a flame ionisation detector (FID). For *n*-alkanes, the oven temperature was programmed from 80 °C to 300 °C at a heating rate of 8 °C/min and the final temperature held for 20 min. A 30-m long DB-5MS fused silica capillary column (0.25 mm i.d., 0.25 μm film thickness) was used for both compound classes. For sterols, the GC oven was programmed from 50°C to 100°C (30°C/min), then from 100°C to 150°C (1.5 °C/min) and to 300°C (3°C/min) held for 20 min. In both cases, a known amount of 5α-cholestane was added to the sample prior GC analysis as an external standard for quantitation. All biomarker sediment concentrations were normalised to TOC.

3.6 H-Print index

In its original work, Brown et al. (2014b) defined HBI-fingerprint as the proportion of seven identified HBIs (in %) produced by pelagic and sympagic diatoms. The first H-Print index was proposed by Brown and Belt (2017) as the ratio of the relative proportion of pelagic and sympagic HBIs. A simplified calculation of H-Print (Eq. 1) was proposed for sediments or marine ecosystems in the Arctic using the three following HBIs (Koch et al., 2020a, b, and 2023; Su et al., 2023) e.g. IP_{25}, HBI II and HBI III determined by GC-MS:

$$H - Print\% = \frac{[HBI-III]}{[IP_{25}]+[HBI-II]+[HBI-III]} \times 100 \qquad (1)$$

Low values of H-Print% are indicative of higher relative sympagic production while high ones reflect prevailing pelagic algae producers. This index was used as an additional information source together with phytosterols to assess phytoplankton production patterns in relation to sea-ice conditions.

3.7 Chlorophyll a analyses

After collection, filters for Chl *a* analysis were extracted with 10 mL of 90% acetone at -20°C in the dark for 24 h and measured using a trilogy laboratory fluorometer (10-AU, Turner Designs), which was calibrated before analysis (Holm-Hansen et al., 1965; Welschmeyer, 1994). The precision of the measurements is 0.02 mg m^{-3}.

3.8 Sea-ice distribution data
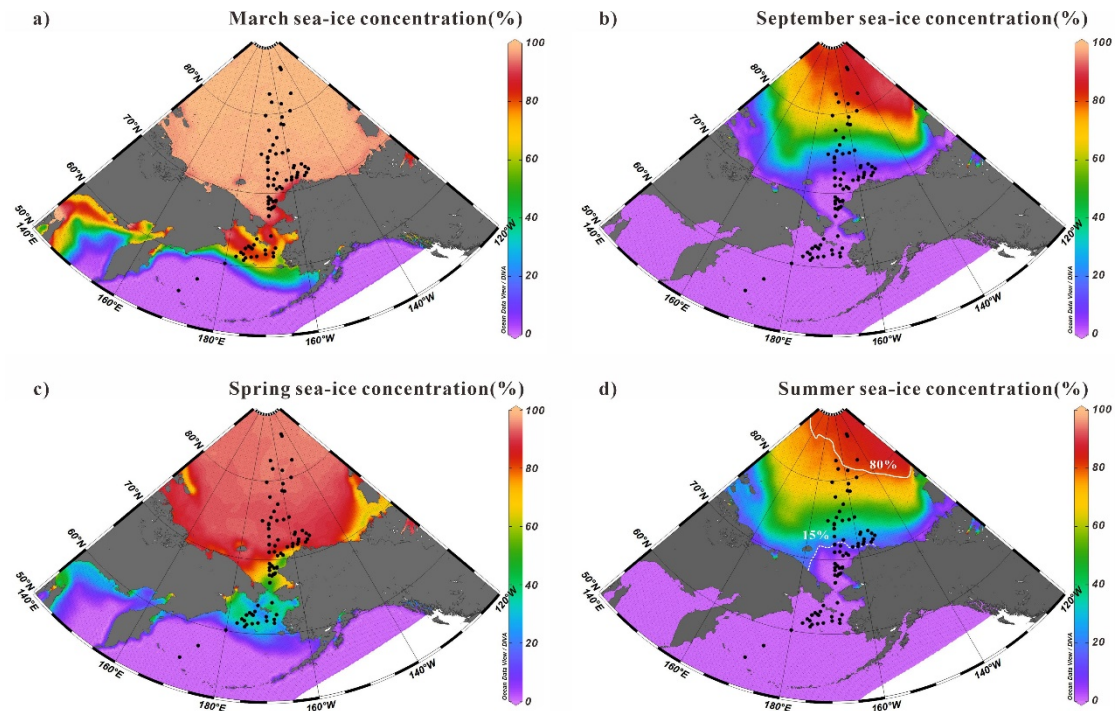
Figure 2. Average sea-ice concentrations in (a) March, (b) September, (c) spring (April, May and June) and (d) summer (July, August and September) from 1994 to 2014 (http://nsidc.org). Black dots are surface sediments samples in this study. The dotted and plain white lines represent the 15% and 80% isolines of summer sea-ice cover for the period 1994-2014.

Satellite sea-ice concentrations in the study region measured from Nimbus-7 SMMR and DMSP SSM/I-SSMIS passive microwave sensors averaged between 1994 and 2014 (Fig. 2a-d). These data were retrieved from the National Snow and Ice Data Center (NSIDC) (DiGirolamo et al., 2022). Fig. 2 shows the seasonal distributions of the sea-ice extent in spring (April-June) and summer (July-September) as well as in March and September. Also shown, are the 15% and 80% isolines that indicate that the summer Ice-Free Zone (IFZ <15% of sea ice) was on average located as far north as 72°N and that the Marginal Ice Zone (MIZ, sea-ice cover from 15% to 80%) reached up to 80°N latitude. However, it must be kept in mind that our surface sediment dataset covers the nearshore, shelf, and basin regions, with different deposition rates. The first 2 cm surface sediments may represent a longer time interval (decades to centuries) than modern satellite data (Pearce et al., 2017; Polyak et al., 2009; Stein et al., 2010).

3.9 Description of ODV

The distributional maps of TOC, TN and biomarker concentrations were generated with the Ocean Data View software package, version 5.6.5 (ODV, odv.awi.de, Schlitzer, 2023). They were created using the DIVA (Data Interpolating Variational Analysis) display styles gridding

for representing sea-ice data from NSIDC and with the coloured dots to visualise biomarker data.

4. Results

4.1 Total organic carbon (TOC) and total nitrogen (TN) in surface sediments

TOC values of surface sediments vary from 0.1 to 2.2% (1.03±0.63%, *n*=52) with highest values localised in the mid-Chukchi Sea Shelf and Bering Sea, and lowest ones at latitudes > 75°N (Fig. 3a) (Table S1). The Bering Strait exhibits relatively low TOC content. The spatial distribution of TN shows similar patterns with values ranging from 0.01% to 0.29% (0.14±0.07%, *n*=50) (Fig. 3b), e.g. one order of magnitude lower than TOC, which results in C/N ratios of about 8 to 10 at all sites except for some northernmost ones that have C/N values roughly two times lower (Fig. 3c).
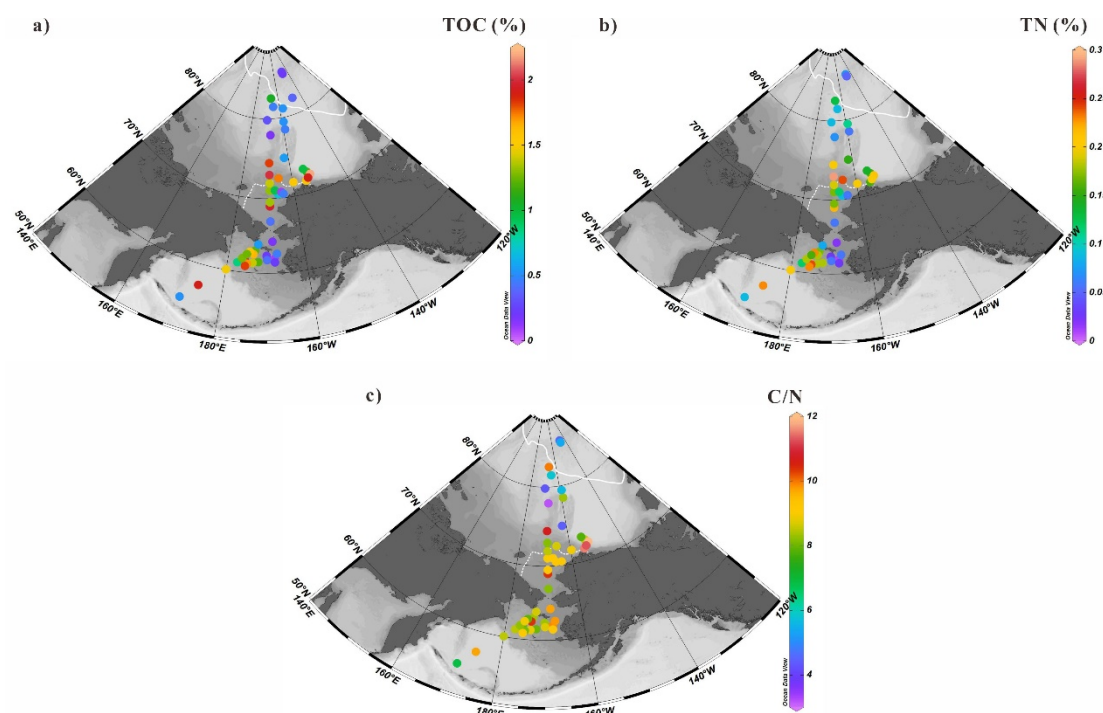
Figure 3. Distributions of (a) Total Organic Carbon (TOC) in %, (b) TN (Total Nitrogen) in % and (c) C/N ratios in the surface sediments from the western Arctic Ocean, the Chukchi Sea and the Bering Sea (this study). For an explanation of dotted and plain white lines, see Fig. 2.

4.2 C$_{25}$ high branched isoprenoid (HBI) alkenes in surface sediments

The sea-ice biomarker IP$_{25}$ was identified in 47 out of the 52 new surface sediments analysed in this study (Fig. 4a). IP$_{25}$ was absent (or below the detection limit) at locations in the Southern Bering Sea or at highest latitude sites between 78°N and 82°N. Concentrations were generally higher in the northeast Chukchi Sea and Barrow Canyon than in the Chukchi Plateau and low in high latitude areas where sea ice is perennial and predominantly ice-free such as at the Bering

Sea slope and shelf (IP$_{25}$: 0.05-1.68 μg g^{-1} TOC, 0.39±0.41μg g^{-1} TOC). HBI-II was also present in most of the sediment extracts (49 out of 52). Its spatial distribution shared similar features as IP$_{25}$ with higher values matching those of IP$_{25}$ (HBI-II: 0.06-3.02 μg g^{-1} TOC, 0.61±0.63 μg g^{-1} TOC; Fig. 4b) and lowest ones at highest latitudes and in most of the Bering Sea sites.

HBI-III was present in 45 out of 52 of the sediment extracts. In contrast to IP$_{25}$ and HBI-II, highest abundance (> 0.17μg g^{-1} TOC) were encountered in the northern Bering Sea and at some sites of the northeast Chukchi Sea where variable sea-ice conditions prevailed in summer (Fig. 2d) and were free of ice in September (Fig. 2b), as expected from HBI-III producers preferably growing in sea-ice edge to ice free waters (0.01-0.94 μg g^{-1} TOC, 0.17±0.22 μg g^{-1} TOC; Fig. 4c). These results are consistent with a pelagic phytoplankton origin for this biomarker (Bai et al., 2019; Belt et al., 2015; Koch et al., 2020a, b; Su et al., 2022) and reflected by H-Print% indicating highest values in the northern Bering Sea gradually decreasing northwards with increasing seasonal sea-ice cover, e.g. lowest value at MIZ about 73°N, slight increase northward from the Chukchi border to high latitudes under extensive sea ice. (Fig. 4d).
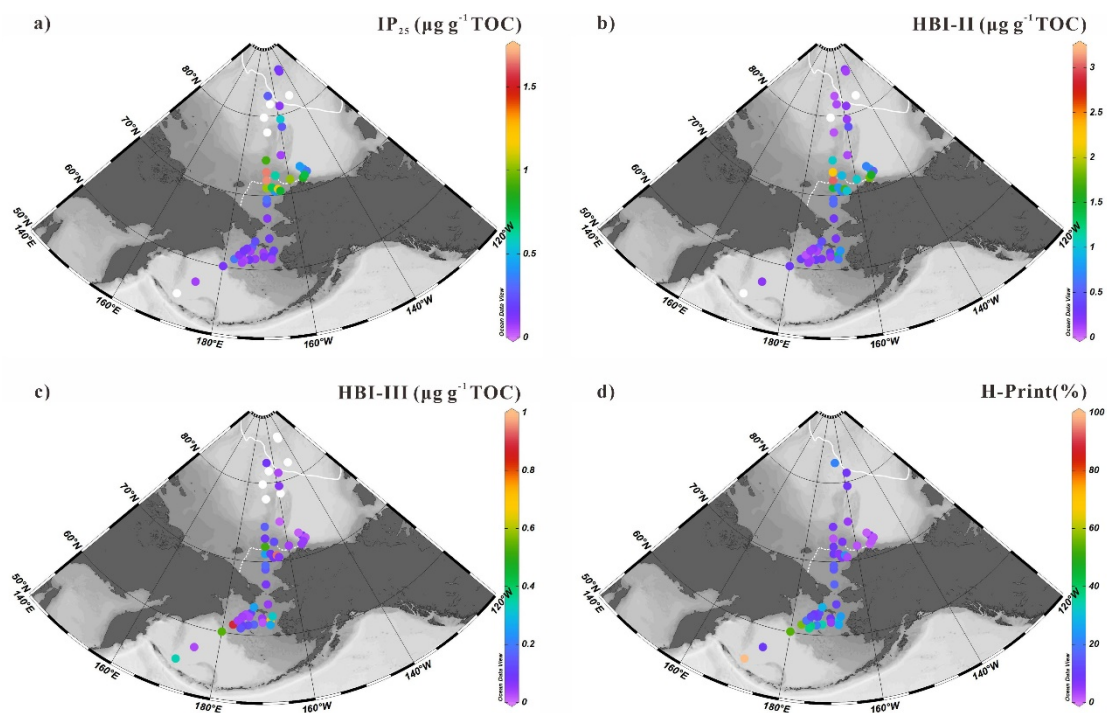
Figure 4. Surface sediment concentrations of HBIs normalized to TOC (expressed in μg g^{-1} TOC): (a) IP$_{25}$, (b) HBI-II, (c) HBI-III; (d) values of H-Print % of the western Arctic Ocean, the Chukchi Sea and the Bering Sea (this study). White dots are sites where HBIs were not detected. For an explanation of dotted and plain white lines, see Fig. 2.

4.3 Sterols in surface sediments

Fig. 5 shows the spatial distribution of prevailing and commonly used sterols in marine settings to identify phytoplankton communities. They include pelagic phytosterols, e.g.

310 brassicasterol (24-methylcholesta-5,22(E)-dien-3β-ol) a common sterol mainly produced by marine diatoms thriving in open-water in the Arctic Ocean though in some case this sterol may also have a riverine/lacustrine algal origin (Fahl and Stein, 1999; Xiao et al., 2015), dinosterol (4α-23,24-trimethylcholest-22(E)-en-3β-ol) mainly synthesized by dinoflagellates but absent in sea ice, campesterol (24-methylcholest-5en-3β-ol) of terrestrial origin and the 24-ethylcholest-

315 5-en-3β-ol, which depending on the configuration of C_{24} that can be of marine (α isomer) or terrestrial (β isomer) origin (Volkman, 2016).

Concentrations of brassicasterol range from 0.72 to 57.67 μg g^{-1} TOC (7.92±10.62 μg g^{-1} TOC) with highest values found in the northern Bering Sea (57.67 μg g^{-1} TOC) and southeastern Chukchi Sea shelf (0.72-37.56 μg g^{-1} TOC) (Fig. 5a). Dinosterol concentrations vary in quite a

320 similar range, from 0.61 to 43.04 μg g^{-1} TOC, around a slightly higher mean value (14.92±11.77 μg g^{-1} TOC). The distribution pattern of dinosterol shows similar features as brassicasterol with high values in the mid- Chukchi Sea shelf and northern Bering Sea but expanding further South (Fig. 5b). Campesterol and 24-ethylcholest-5-en-3β-ol show high values notably along the coast of Alaska and decrease off-shore across the Bering Strait (campesterol: 0.47-123.41 μg g^{-1} TOC

325 (30.88±31.36 μg g^{-1} TOC); 24-ethylcholest-5-en-3β-ol ranges from 0.67 to 152.35 μg g^{-1} TOC (39.52±42.08 μg g^{-1} TOC)) (Fig. 5c, d). These sterols were also both present at low levels at lowest and highest latitudes.
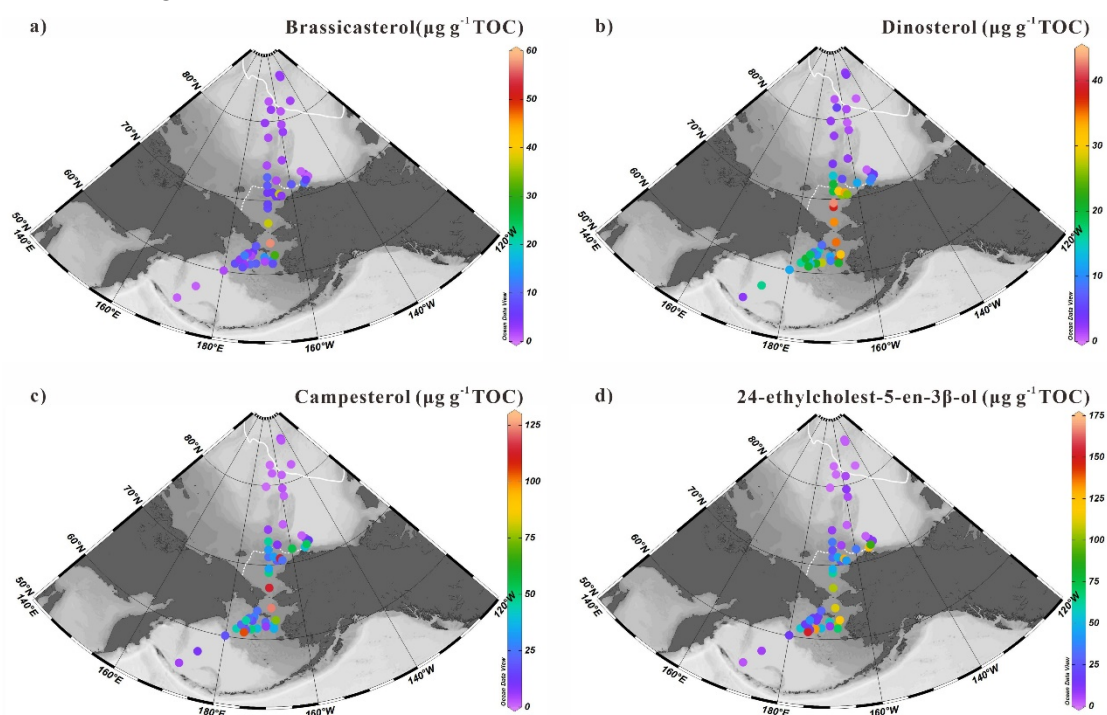
Figure 5. Concentrations of sterols expressed in μg g^{-1} TOC: (a) brassicasterol, (b) dinosterol,
330 (c), campesterol and (d) 24-ethylcholest-5-en-3β-ol in surface sediments from the western Arctic Ocean, the Chukchi Sea and the Bering Sea (this study). For an explanation of dotted and plain white lines, see Fig. 2.

4.4 N-alkanes in surface sediments

335   The homologous distribution of *n*-alkanes in our sediments display an odd-to-even predominance characteristic of epicuticular waxes produced by higher plants (Yunker et al., 1995). The sum of the concentrations of high molecular weight odd carbon numbered chain *n*-alkanes (C_{27}, C_{29} and C_{31}) was calculated to assess terrestrial inputs to surface sediments. The $\sum C_{27}$-C_{31} values shown in Fig. 6 vary from 11.67 to 211.86 µg g^{-1} TOC (84.16±43.44 µg g^{-1}

340   TOC) with higher contents in the southeastern Chukchi Sea shelf across the Bering Strait till the North Bering Sea. Moderate values (>100 µg g^{-1} TOC) were found at some sites of the High Arctic.
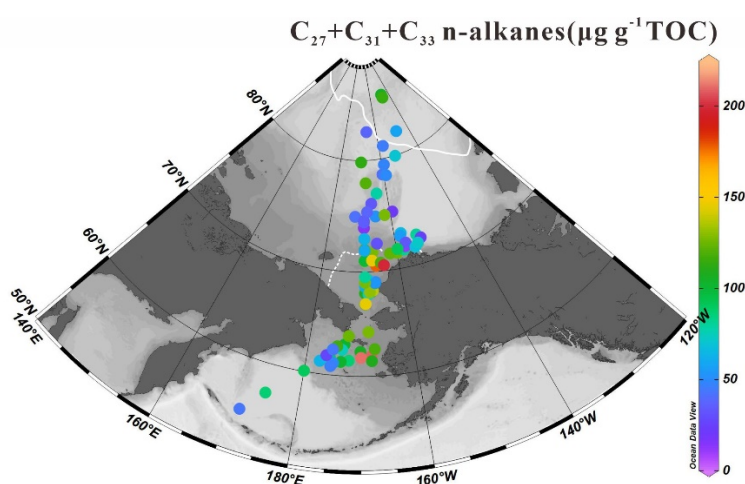
Figure 6. Sum of terrigenous long-chain odd numbered C_{27}+C_{29}+C_{31} *n*-alkanes (expressed in
345   µg g^{-1} TOC) in surface sediments (*n*=88) from the western Arctic Ocean, the Chukchi Sea and the Bering Sea (this study). For an explanation of dotted and plain white lines, see Fig. 2.

4.5 Sterols and Chl a in surface suspended particles

Fig. 7 shows the sterol concentrations measured in surface suspended particles collected at
350   13 stations located along a latitudinal transect between 68.6°N and 79.4°N (orange triangles in Fig. 1 and Fig. 7f). They include brassicasterol, dinosterol, 24-ethylcholest-5-en-3β-ol and cholest-5-en-3β-ol (cholesterol). Note that neither HBIs nor campesterol were detected in SPM samples indicating their absence or trace levels, below the detection limit. Concentrations of brassicasterol ranged from 0.80 to 132.31 ng L^{-1}, 17.11±37.46 ng L^{-1}) (Table S3) with highest

355   values found in the mid-Chukchi Sea shelf where Chl *a* also reached highest values and lowest ones North of 75°N (Fig. 7a). Dinosterol concentrations range in a much lower range from 0.51 to 17.11 ng L^{-1} (4.07±5.39 ng L^{-1}) and display similar trends as brassicasterol (Fig. 7b). Likewise, 24-ethylcholest-5-en-3β-ol also shows increased concentrations southwards spanning from 1.88 to 46.04 ng L^{-1} (9.11±12.13 ng L^{-1}) (Fig. 7c). Finally, cholesterol, one of the most abundant

360   sterols in SPM, varied from 1.20 to 117.29 ng L^{-1} (17.02±32.04 ng L^{-1}) in a range that is similar to brassicasterol (Fig. 7d). Despite possible algal sources, cholesterol is considered to be mainly

reflecting the presence of zooplankton as it converts much of the sterols produced by algae into cholesterol. Chl a in surface waters show the same South to North latitudinal decrease with concentrations spanning from 0.05 to 5.40 mg/m^3 (0.69 ±1.66 mg m^{-3})(Fig. 7e).
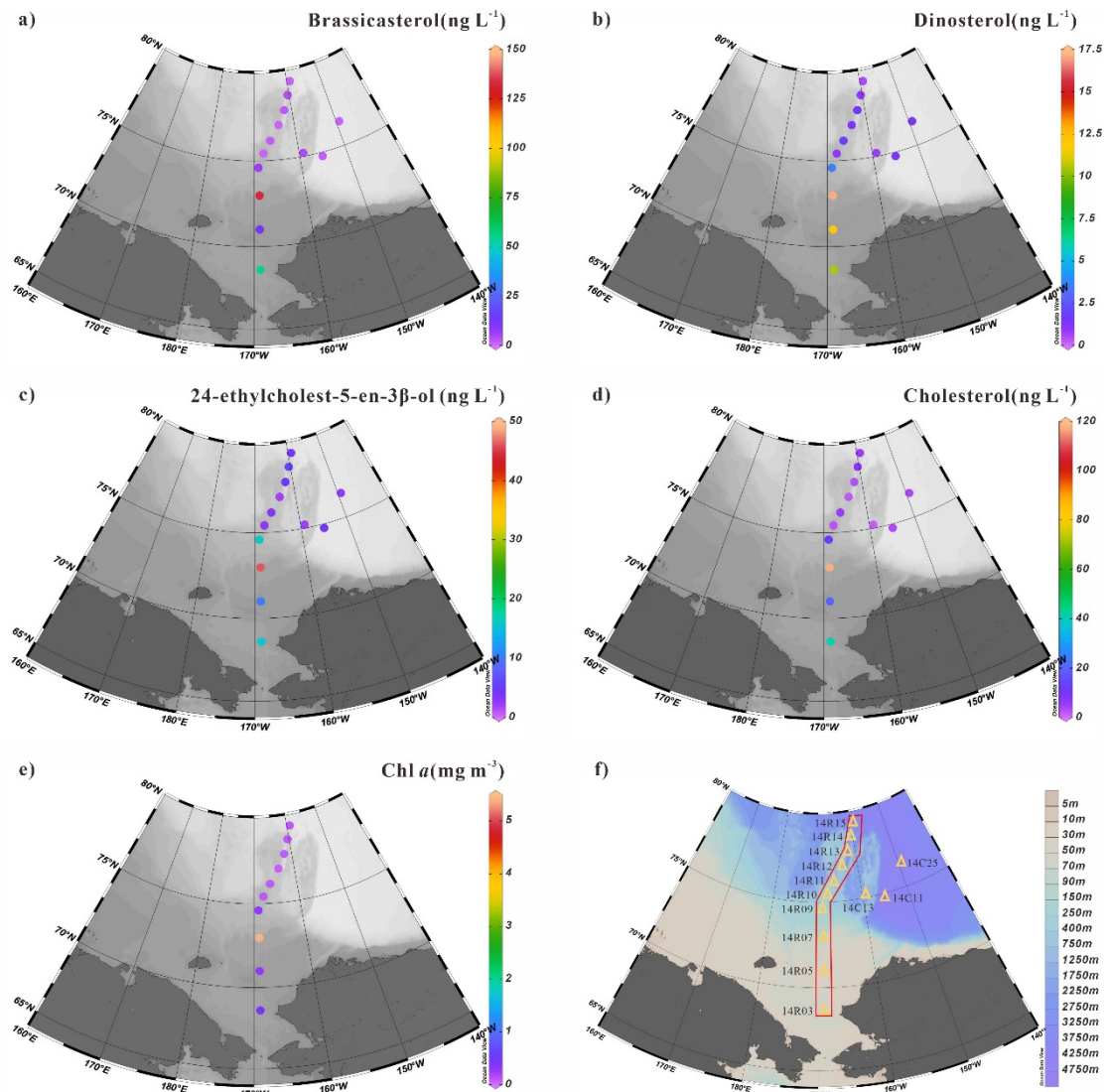
Figure 7. Distribution of biomarker sterols (in ng L^{-1}) and chlorophyll a (in mg m^{-3}) in surface suspended particles collected in summer 2014:(a) brassicasterol, (b) dinosterol, (c) 24-ethylcholest-5-en-3β-ol, (d) cholesterol, (e) Chl a. (f) transect showing the 10 out of 13 stations from the shelf to the basin in the Chukchi Sea where suspended particulate matter was collected.

5. Discussion

5.1 Impact of sea ice on sedimentary HBIs distribution

In this section, we discuss the spatial distribution of HBIs based on the compilation of the sedimentary data from the CHINARE cruises ARC3, ARC4, ARC5 and ARC6 in the Chukchi Sea and Bering Sea (this study) and those from the CHINARE cruises ARC3, ARC5 and ARC6 published by Bai et al. (2019) obtained following the same analytical procedure (Fig. 8).
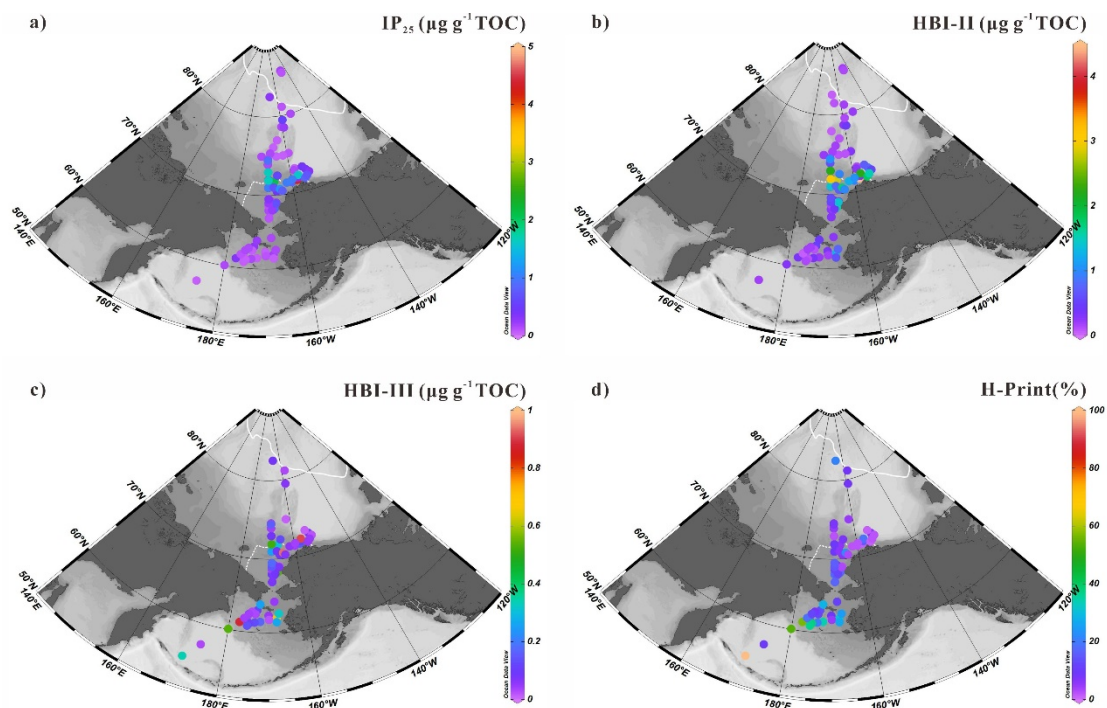
Figure 8. Surface sediment concentrations of HBIs normalized to TOC (expressed in µg g^{-1} TOC): (a) IP$_{25}$, (b) HBI-II, (c) HBI-III ; (d) values of H-Print % in the sites (*n*=88) of the western Arctic Ocean, the Chukchi Sea and the Bering Sea. For an explanation of dotted and plain white lines, see Fig. 2.

Sympagic IP$_{25}$ and HBI-II values of the combined data set range from 0.05 to 4.39 µg g^{-1} TOC (0.45±0.61 µg g^{-1} TOC) and from 0.06 to 4.46 µg g^{-1} TOC (0.66±0.75 µg g^{-1} TOC), respectively (Fig. 8a-b, Tables S2). These values are close to those reported by Bai et al. (2019) spanning from 0.09 to 4.39 µg g^{-1} TOC (0.52±0.80 µg g^{-1} TOC) and from 0.12 to 4.46 µg g^{-1} TOC (0.72±0.89 µg g^{-1} TOC) for IP$_{25}$ and HBI-II, respectively. They confirm the extreme values off the Alaskan coast and provide new lower extremes in the Bering Sea slope and shelf, not included in the study of Bai et al. (2019), where ice free conditions prevail in summer (Fig. 8a-b). The strong correlation between sedimentary IP$_{25}$ and HBI-II (r^2= 0.87, p<0.05, Fig. S1) agrees with these two structural homologues having common sources in the Arctic Ocean and northern North Atlantic (Belt, 2018) and with the presence of HBI-II in each all IP$_{25}$-producing species studied by Brown et al. (2014a). Overall, the distribution patterns of sympagic IP$_{25}$ and HBI-II in the augmented dataset confirms the earlier finding of low values at latitudes >73°N due to extensive sea-ice cover in summer and provide new low end-member values South of the Bering Strait essentially free of ice in summer. Enhanced sympagic production is generally found on the path of the warm polar wards PW and ACW flowing along the coast of Alaska both contributing to ice melting. Comparison with other published data shows that our IP$_{25}$ values are lower than reported in the Chukchi Plateau and basin by Xiao et al. (2015), lying between 0.63 and 8.97 µg g^{-1} TOC, a result that is explained by the generally more northern position of their sites and possibly also different quantification methods. Lowest IP$_{25}$ reported

by Méheust et al. (2013) (0.079 to 0.567μg g^{-1} TOC) in a few (3 out of 11) surface sediments of the Bering Sea are also in agreement with our results and expected from seasonal sea ice in the Bering Sea shelf break, North of the March sea-ice edge (20% isoline in Méheust et al., 2013). The northward latitudinal decrease of IP$_{25}$ in surface sediments and elevated values around 70°N were also reported by Koch et al. (2020a).

The distribution pattern of pelagic HBI-III is expectedly different from that of sympagic HBIs and exhibit much lower abundances (0.01 to 0.94 μg g^{-1} TOC, 0.16±0.21μg g^{-1} TOC) (Fig. 8c, Table S2). HBI-III is absent or present in trace amounts mostly in ice-covered areas of the High Arctic and highest at summer ice-free sites of the northern Bering Sea (Station 10BB01, 0.89 μg g^{-1} TOC, Table S2). Elevated concentrations occurred in the southeastern Chukchi Sea shelf along the coast of Alaska, as also found by Koch et al. (2020a), and in the Bering Sea. These observations translate into H-Print index values indicating that pelagic to sympagic diatom production and export increases from North to South across the Bering Strait and further in the northern Bering Sea (Fig. 8d). This result is consistent with previous finding in the Pacific Arctic surface sediments by Koch et al. (2020b).

Advective processes linked to the PW flow and their impact on sea-ice dynamics in shaping algal communities have been invoked to explain sympagic to pelagic spatial distribution. The rate of sea-ice retreat in the Chukchi Sea is closely connected to heat transport by the PW triggering the onset of sea-ice melting in spring/summer. Time series from a year-round mooring deployed in the Bering Strait has shown that annual mean transport volume of PW increased by ~70% between 2001 and 2014 (Woodgate, 2018). Woodgate and Peralta-Ferriz (2021) further calculated an increase of 0.1 Sv/yr between 1990 and 2019 and a corresponding ~0.1°C/yr warming in spring/summer over this time interval. These authors also outlined that concomitantly the warm period extended from 5.5 to 7 months. This is in contrast with the Bering Sea that does not show any significant long-term reduction since 1850, despite a general warming climate, but pronounced decadal scale variability (Walsh et al., 2017) driven by the Pacific Decadal Oscillation (PDO), the dominant mode of atmospheric variability in the North Pacific.

Overall, based on HBI sedimentary distribution and their translation into H-Print, we were able to discriminate the three following sub-regions (Fig. 9) : I) the Bering Sea characterized by high variability of pelagic to sympagic production reflecting a wide range of sea-ice conditions with sea ice forming in winter and ice-free conditions in summer (Walsh et al., 2017), II) the productive MIZ waters of the mid-Chukchi Sea shelf with higher sympagic production and export, and lower spread associated with variable seasonal sea-ice conditions, III) the slope and western Arctic Ocean basin characterized by dominating sympagic production and slightly less variability reflecting prevailing high sea-ice cover.
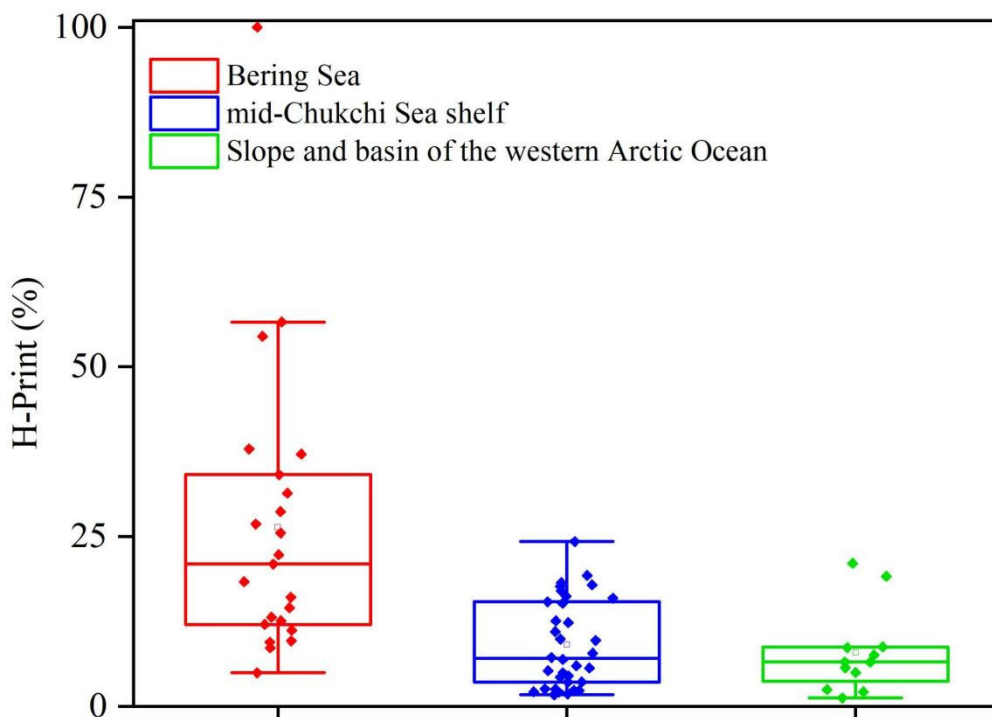
Figure 9. Boxplot of H-Print index in surface sediments from the Bering Sea (in red), mid-Chukchi Sea shelf (in blue) and the slope and western Arctic Ocean basin (in green).

5.2 Latitudinal variations of sympagic to pelagic phytoplankton production

In order to explore further the relationship between the icescape and sympagic to pelagic production across the wide range of sea-ice situations encountered from the Bering Sea to the High Arctic Ocean, phytosterols (brassicasterol+dinosterol) in surface sediments were investigated and compared with spring and summer sea-ice concentrations provided by the NSIDC (Fig. 10a). As shown in Fig. 10b, sympagic production increased from 62°N to 70°N to reach maximum values near the sea-ice edge and MIZ, between 70°N and 73°N, and decreased to low values similar to the IFZ at latitudes >73°N as sea ice became permanent. In contrast, enhanced pelagic phytosterols and HBI-III largely prevailed in open waters of the Bering Sea in spring and summer and decreased relative to sympagic production in the MIZ demonstrating a progressive transition of habitats.
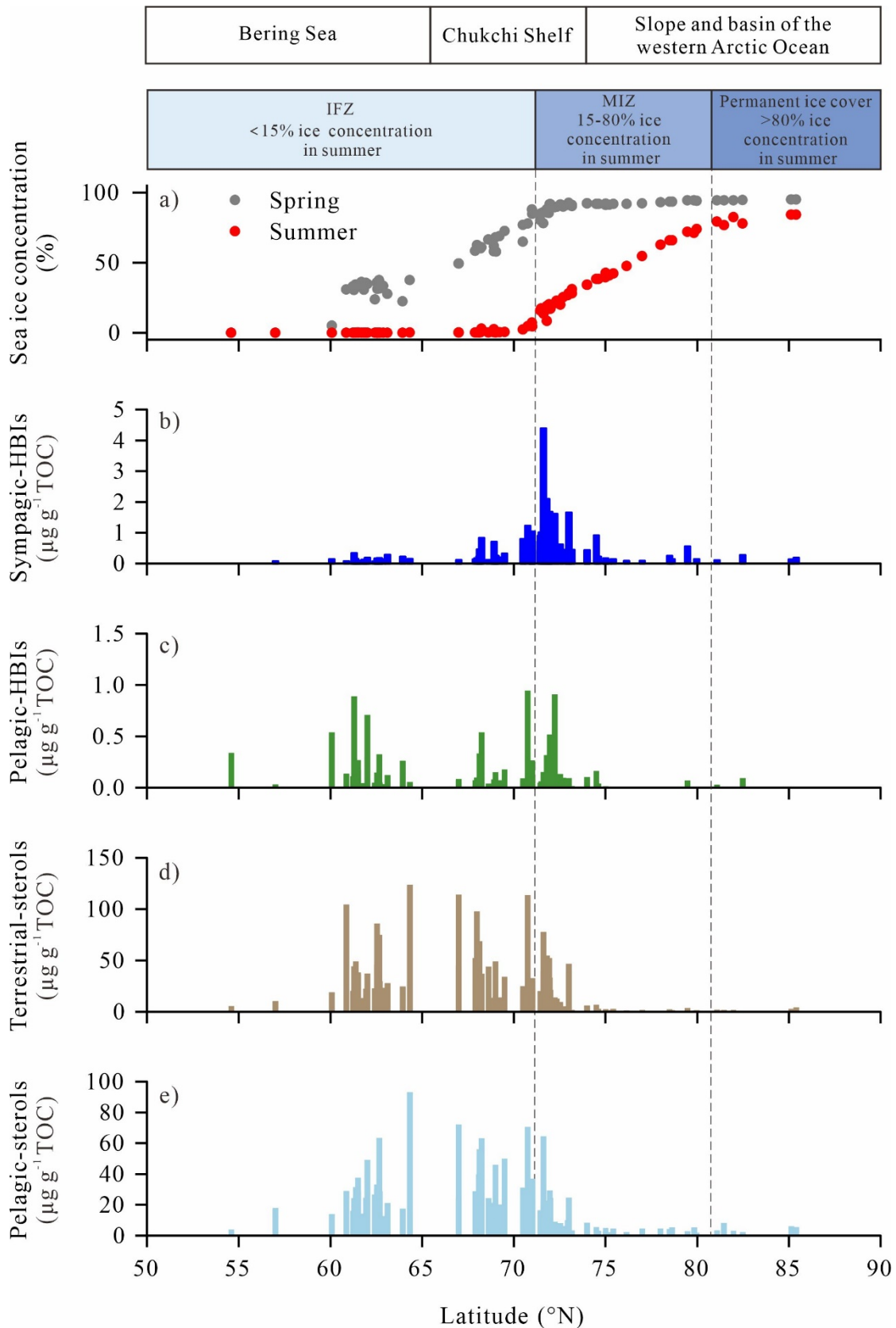
Figure 10. Concentrations of (a) spring and summer sea ice (in %) for the period 1994-2014 retrieved from NSIDC, (b) sympagic HBIs (IP$_{25}$, in µg g^{-1} TOC) ,(c) pelagic HBIs (HBI-III, in µg g^{-1} TOC), (d) terrestrial sterol (campesterol, in µg g^{-1} TOC), (e) pelagic sterol (brassicasterol+dinosterol, in µg g^{-1} TOC) in surface sediments along the latitudinal transect from the Bering Sea to the western Arctic Ocean.

This biogeographic pattern is supported by surface sediment data of Koch et al. (2020a) retrieved from the Distribution Biological Observatory (DBO) regions surveyed during several cruises from 2012 to 2017 (Moore and Grebmeier et al., 2018) where abundances of IP_{25} in the northeast Chukchi Sea and Barrow Canyon (71-72.5°N) prevailed over those of lower latitudes (62-68°N). Although the specific source of HBI-III in Arctic Ocean sediments have not been identified unequivocally, high pelagic HBI-III values in IFZ and MIZ (Fig. 10c) are in agreement with the only known producer marine diatoms of the genera *Rhizosolenia and Pleurosigma* living at sea-ice edge or ice-free waters (Belt et al., 2017; Belt, 2018; Koch et al., 2020a; Smik et al., 2016). Consistent with our results, enhanced HBI-III has also been reported in surface sediments of the Barents Sea underlying the minimum and maximum April sea-ice margin (Belt et al., 2015). Further evidence was provided by sediment trap time-series showing peaking HBI-III export flux at low sea ice/sea-ice retreat at the station in the Chukchi Sea slope (Bai et al., 2019; Gal et al., 2022). Dominant pelagic production in the northern Bering Sea is consistent with expanded open water areas and lengthened phytoplankton growing season compared to more northern locations. Sea-ice thinning and melting are key factors responsible for increased primary production and northwards expansion of phytoplankton blooms over the last decades (Renaut et al., 2018). Physical modelling also evidenced a clear northward shift of phytoplankton blooms from the Bering Sea to the Arctic shelf in the western Arctic Ocean with decreasing sea ice (Jin et al., 2012). Kahru et al. (2016) estimated an increase by 47% of the net primary production across the Arctic Ocean between 1998 and 2015 in the spring and summer. These changes are largely due to enhanced incoming light resulting from earlier ice breakup in summer, later freezing in winter, increased open water areas and a longer ice-free season boosting the phytoplankton production. In some areas, spring blooms along the sea-ice edge contribute more than half of the annual primary production and fall bloom becomes more frequent at latitudes >70°N (Ardyna et al., 2014). Other dynamical factors linked to the decline of sea ice can contribute to increase primary production such as wind-driven mixing and upwelling both leading to the replenishment of surface waters with nutrients in the Chukchi Sea continental shelf (Huntington et al., 2020; Pickart et al., 2011). However, freshening associated with sea-ice melting and subsequent ocean stratification counteract these processes by reducing nutrient availability in surface waters in summer-early fall. Finally, the PW represents a major source of nutrients for phytoplankton growth across the Bering Strait and along the coast of Alaska, which also allows the intrusion of temperate species in the Arctic Ocean (Ardyna and Arrigo, 2020).

Pelagic phytosterols (e.g. brassicasterol and dinosterol) along our latitudinal gradient share strong resemblance with HBI-III but show higher values relative to HBI-III in the IFZ, e.g. in

the southern Chukchi shelf between 68 and 70°N (Fig. 10,c-e). At latitudes >81°N, on the slope and western Arctic basin under perennial sea ice, pelagic phytosterols drop to their lowest

495   levels as a result of light and nutrient limitation (Fernández-Méndez et al., 2015; Gosselin et al., 1997). This result suggests that diatom production below sea ice is not significant at these extreme latitudes probably because of sea-ice thickness preventing light transmission as also revealed by the OC and TN contents of the sediments (Arrigo et al., 2012, Coupel et al., 2012).

Interestingly, campesterol displays broadly similar features as phytosterols with higher

500   values found across the Bering Strait, at the northern Bering Sea and on mid-Chukchi Sea shelf (Fig. 10d). The occurrence of branched and isoprenoid tetraethers in surface sediments in the Bering Sea and inner shelf of the Chukchi Sea (66-73°N) (Park et al., 2014) as well as $\delta^{13}C$ values < -25‰ (Grebmeier et al., 2006; Ji et al., 2019; Naidu et al., 2004) further support a higher contribution of land-derived inputs to the sediments that is also reflected by our C/N

505   values (Fig. 11c, d). Using the BIT index as a proxy of terrestrial carbon, Park et al. (2014) reported low values on the outer shelf of the Chukchi Sea (73-75°N), moderate values offshore the Bering Sea, inner shelf of the Chukchi Sea (66-73°N) and western Arctic Ocean north of 75°N, and highest values in the Yukon and Mackenzie River estuaries. With the loss of continental ice, increasing temperature and precipitation, enhanced biomass production on land

510   and intensified erosion have resulted in increased river discharge of suspended particulate matter in the coastal Arctic Ocean. Change in sea-ice distribution also influences terrestrial inputs to the sediment, through ice drifting from coastal areas (Darby et al., 2009; Eicken et al., 2005). Note that higher plant n-alkanes (Fig. 6) show no latitudinal trend and unexpectedly high values in the High Arctic that demonstrate that allochthonous material reaches the central Arctic

515   Ocean. The north-west Bering Sea higher value area might be contributed by the Yukon River (Brabets et al., 2000), while high values in the southeastern Chukchi Sea shelf might be contributed by near-shore sea-ice transport, which bring massive black sediments when they formed in near shore close to Barrow (Darby et al., 2009; Harper, 1978).

5.3 Comparison of sterols in suspended particles with surface sediments

520   Biogeochemical data in the water column escapes satellite measurements and are thus very scarce and critically needed to fully understand the impact of on-going changes on primary production and the export and sequestration of organic carbon in the Arctic Ocean. As discussed in the previous sections, surface waters properties are very sensitive to environmental changes linked to sea ice that exerts a strong control on primary producers and ultimately food resources

525   (Lannuzel et al., 2020). The amount of exported organic material to the deep ocean depends on the structure of the phytoplankton community and subsequent higher trophic levels (Leu et al., 2011). The mismatch of spring phytoplankton bloom and zooplankton grazing activity caused by earlier sea-ice melting and earlier blooming could lead to lower consumption of

phytoplankton by grazing heterotrophs in the water column thereby also affecting export (Hunt
et al., 2002; Søreide et al., 2010). In this section we investigate the sterols in suspended particles
and underlying surface sediments to assess vertical transport pathways, though on a limited
sample set.
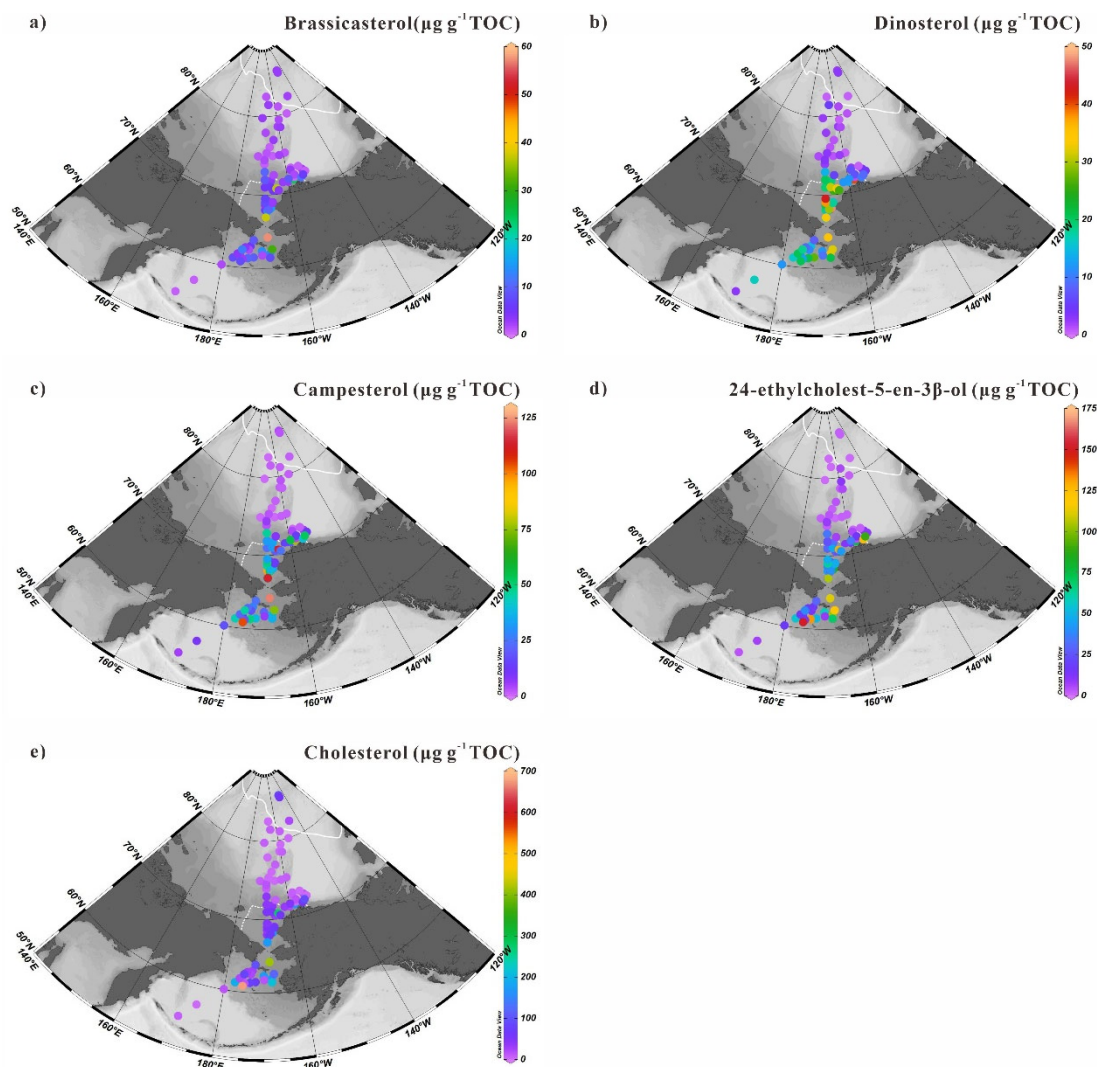
Figure 11. Concentrations of sterols normalized to TOC in surface sediments (expressed in µg
g^{-1} TOC): (a) brassicasterol and (b) dinosterol; (c) campesterol and (d) 24-ethylcholest-5-en-
3β-ol; (e) cholesterol in the surface sediments (*n*=88) from the western Arctic Ocean, the
Chukchi Sea and the Bering Sea. For an explanation of dotted and plain white lines, see Fig. 2.

As earlier outlined, higher contents of brassicasterol and dinosterol are localized in surface
sediments of the Bering Sea shelf and the southeastern Chukchi Sea shelf and decreased sharply
around 73°N to the North with increasing sea-ice cover (Fig. 11a,b). Despite the limited SPM
sample set, brassicasterol and dinosterol in SPM reproduce the northward decrease with
increasing sea ice similar as Chl *a* with highest values found in the South of Chukchi Sea shelf
(Fig. 7). The correlation between 24-ethylcholest-5-en-3β-ol and Chl *a* is significant (r^2=0.90,
p<0.05) (Fig. S2) and remains high even after the removal of the most extreme value (r^2=0.79,

545 *p*<0.01) (Fig. S3) pointing out a prevailing contribution of the marine origin α isomer 24(α)-ethylcholest-5-en-3β-ol over the β isomer, β-sitosterol, as reported Tolosa et al. (2013) who demonstrated the prevalence of 24(α)-ethylcholest-5-en-3β-ol even in coastal waters of the southeast Beaufort Sea. These observations are also in line with minor amounts or below the detection limit of terrestrial biomarkers e.g. campesterol and *n*-alkanes in SPM.

550 Cholesterol is usually a dominant sterol in zooplankton (Volkman, 1986) and has often been considered as an indicator of zooplankton activity (Grice et al., 1998), although this compound can also be produced by some algal species. Higher cholesterol abundances were essentially found in northern Bering Sea sediments (Fig. 11e). In suspended particles, linear regression led to correlation coefficients (r^2) of 0.99 and 0.79 (both *p*>0.05) for cholesterol against

555 brassicasterol and for cholesterol against dinosterol (Fig. S4). In contrast, for sediments, the statistical relationships between cholesterol and brassicasterol or cholesterol and dinosterol (r^2=0.37, *p*<0.01 and r^2=0.27, *p*<0.01, respectively; Fig. S5), are weak. Yet, phytoplankton and zooplankton living below sea ice and in the subsurface chlorophyll maximum e.g. deeper depth than 5m (our sampling depth) are not accounted in the SPM, while they may represent an

560 important component of primary production and exported material to the sea floor (Arrigo et al., 2012; Coupel et al., 2012). The timing of phytoplankton bloom and zooplankton grazing is another factor that could account for this discrepancy.
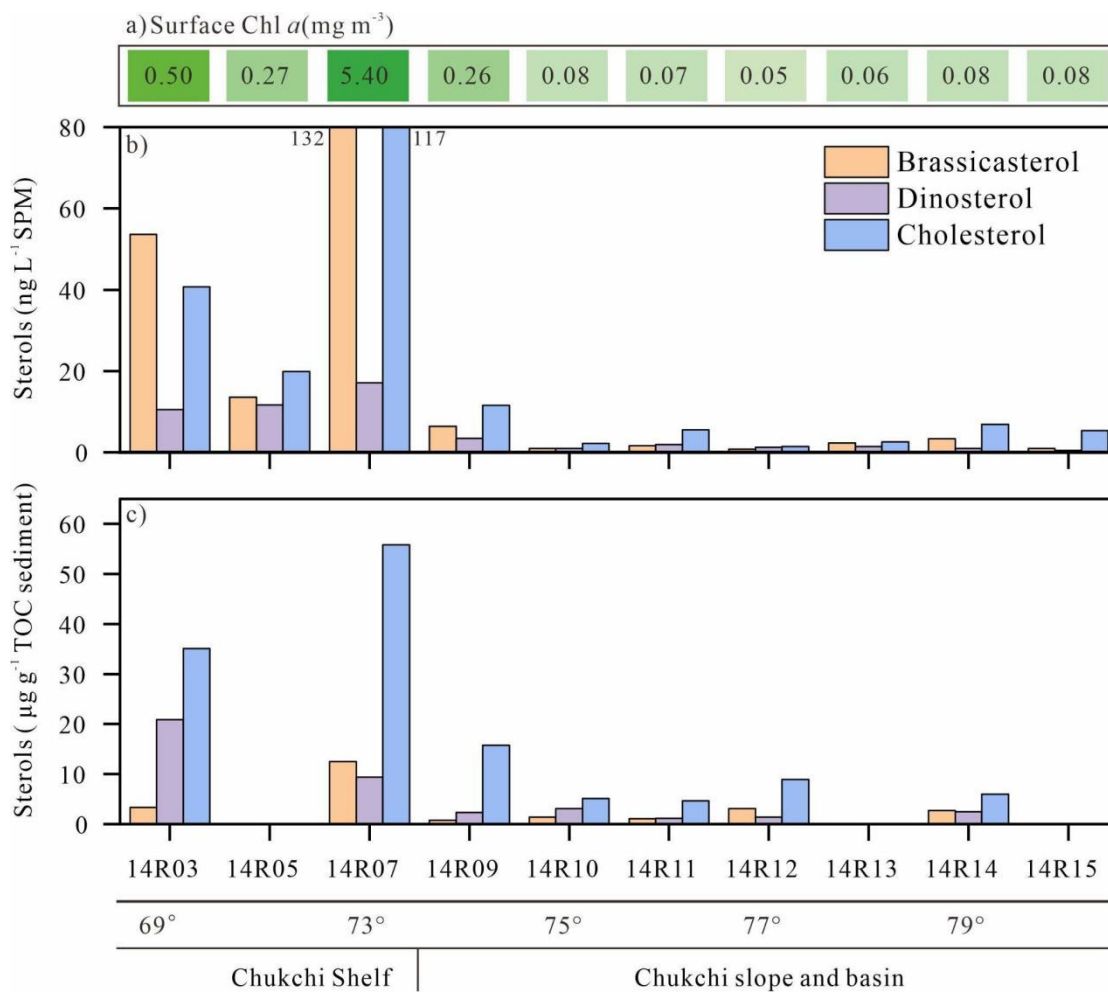
Figure 12. Concentrations in surface waters of Chl *a* (a) brassicasterol, dinosterol and cholesterol in SPM (b) and underlying surface sediments (c) along the transect from the shelf to the basin in the Chukchi Sea. For location of the transect see Fig.7. Please note that there is no sediment sample at 14R05, 14R13 and 14R15.

Table 1 Ratios calculated from individual sterol concentrations in suspended particulate matter (SPM) and sediments from the Chukchi shelf and slope and basin of the western Arctic Ocean.

	14R03	14R05	14R07	14R09	14R10	14R11	14R12	14R13	14R14	14R15
SPM										
B/C	1.32	0.68	1.13	0.55	0.42	0.30	0.54	0.86	0.48	0.19
D/C	0.26	0.59	0.15	0.30	0.42	0.34	0.84	0.55	0.14	0.09
B/D	5.10	1.16	7.73	1.84	1.01	0.89	0.65	1.55	3.51	1.95
Sediment										
B/C	0.10	—	0.22	0.05	0.27	0.23	0.35	—	0.45	—
D/C	0.60	—	0.17	0.15	0.60	0.24	0.15	—	0.41	—
B/D	0.16	—	1.34	0.32	0.44	0.94	2.26	—	1.11	—

Sterol: (B) brassicasterol (24-methylcholesta-5,22E-dien-3β-ol), (C) cholesterol (cholest-5-en-3β-ol), (D) dinosterol (4α, 23,24R-trimethyl-5α-cholest-22E-en-3β-ol).

575   Fig. 12 shows the cholesterol and phytosterol concentrations in SPM and underlying surface
sediments along a latitudinal transect between 69°N and 79°N latitude. Sterols and Chl a both
exhibit large amplitude change in surface waters and underlying surface sediments from North
to South. Highest brassicasterol and Chl a in surface waters of the northern Chukchi shelf at
station 14R07 reflect the highly productive waters, underlined earlier in the discussion, with a

580   major contribution of diatom pigment fucoxanthin (Fig. 12a-b, Table S1). Zhuang et al. (2020)
reported high biomass of diatoms (>20 μm) dominating in the subsurface chlorophyll maximum
during the same cruise in summer 2014, South and North of the Chukchi shelf. This hotspot of
primary production is sustained by continuous nutrient supply by the PW both during the ice
melting season and ice free season. The second highest Chl a and brassicasterol values of the

585   transect are found at the southern site 14R03 bathed by low nutrients Alaska Coastal Water that
indicate the dominance of small diatoms (< 20 μm) (Zhuang et al., 2020). To the North beyond
the shelf, in the Chukchi slope and basin, SPM and sediments display lowest Chl a and sterol
values but shows that primary production is still significant beyond the continental shelf.
Similarly, Gosselin et al. (1997) reported that both phytoplankton and ice algal production were

590   highest over the Chukchi shelf (70°-72° N) and decreased polewards with increasing sea-ice
cover and/or the depth of the surface mixed layer, both determining the light and nutrient
available to microalgae growth. Arrigo et al. (2012) found massive under-ice phytoplankton
bloom over the Chukchi shelf around 73°N supported by light transmission through first-year
ice (0.8-1.3 m in thickness) due to thinning sea ice and proliferation of melt ponds. Dominating

595   brassicasterol over dinosterol in surface SPM in the Chukchi shelf (stations 14R03, 14R05 and
14R07) indicate diatom-rich waters in the MIZ (Table 1). However, underlying sediments
evidence limited export of brassicasterol compared to dinosterol suggesting efficient grazing of
diatoms and their transfer in the food web. At the southernmost station 14R03, phytoplankton
in surface waters was dominated by small diatoms that are more inclined to remain and degrade

600   in the upper layer, because they can hardly sink if not grazed (Table S1). Another explanation
for different vertical transport is that 14R03 experienced ice free and stratified conditions in
summer that favour dinoflagellates development late in the season and their more efficient
export to surface sediments while diatoms seem to be mostly consumed early in the spring
bloom season. High cholesterol abundances in mid-Chukchi Sea shelf SPM and underlying

605   sediments reflect the consumption by herbivorous zooplankton and export through faecal
pellets in the richest phytoplankton waters (Fig. 12b-c). It also underlines the preservation of
organic matter in shallow depth sediments of the Chukchi shelf. With the exception of site
14R05, for which sediment data are missing, these finding are illustrated by brassicasterol/
cholesterol ratios (B/C) mainly >1 and highly variable in the SPM over the Chukchi shelf, and

610   B/C<1 in the Chukchi slope and basin (Table 1). Prevailing cholesterol in surface sediments

associated with B/C<1 and D/C<1 further emphasizes the role of zooplankton and grazing pressure on primary producers in the rich waters of the MIZ and likely efficient transfer to higher trophic levels.

6. Conclusions

Using the HBI biomarkers and H-Print sea-ice index of 88 surface sediments distributed along a latitudinal transect from the Bering Sea till the High Arctic, we were able to distinguish three biogeographic regions: i) the Bering Sea exhibiting a high variability of enhanced pelagic to sympagic production reflecting a wide range of sea-ice conditions of the IFZ more strongly influenced by the PDO than global warming, ii) the mid-Chukchi Sea shelf productive waters characterized by higher and less variable sympagic production due to variable sea-ice conditions of the MIZ, and iii) the slope and western Arctic Ocean basin displaying higher sympagic relative to pelagic production constrained by a higher sea-ice cover and narrow variability. Our results also underline the role of PW inflow in shaping local environmental changes and primary production in the mid-Chukchi Sea shelf located in the MIZ through heat and nutrient transport.

Our data evidence a conspicuous latitudinal trend in phytoplankton population with increasing sympagic relative to pelagic production northward and highest production and export of both sea-ice microalgae and pelagic diatoms in the MIZ in the mid-Chukchi continental shelf. Low terrestrial sterols and *n*-alkanes in surface sediments underscore a low terrigenous contribution to the sediments with no clear latitudinal trend highlighting different sources and transport pathways than marine organic matter. This is further confirmed by their absence or below detection level in suspended particles between 68.6°N and 79.4°N. Quite unusually, we also found that the 24-ethylcholest-5-en-3β-ol was essentially represented by the marine α-isomer, the 24(α)-ethylcholest-5-en-3β-ol, even at most coastal sites.

Comparison of phytosterols and cholesterol fingerprint between SPM and surface sediments suggest efficient consumption of ice microalgae and pelagic diatoms during the spring blooms as compared to dinoflagellates that generally thrives under stratified conditions towards the end of the production season. However, more investigation in the water column and of the sinking particle flux is needed to get a comprehensive picture of the fate and behavior of phyto- and zooplankton. An integrated approach combining trophic biomarkers such as fatty acids and carbon stable isotopes, could serve as a basis to explore further the links between phyto- and zooplankton in this complex environment and improve our understanding of the fate of sea-ice algae and pelagic production and their dynamics across the food web. This knowledge is essential to evaluate the future evolution of marine resources for local populations as well as for assessing the amount of OC transferred and sequestered to the sea floor to also advance our

understanding of carbon cycle feedback mechanisms on climate in this rapidly changing Pacific Arctic system.

650 **Data availability**

All data that support the findings of this study are included with the article (and supplementary information files).

Author contributions

655 Y. B. and J. C. designed the study. M.-A. S. initiated the writing of the paper with Y. B. J. R. for reviewing the paper. V. K. contributed the biomarker analyses (HBIs and sterols) and paper content. H. J. acquired funding from Chinese Arctic and Antarctic Administration and made edits on the final version.

660 **Competing interest**

The authors declare that they have no known competing financial interests or personal relationships that could have appeared to influence the work reported in this paper.

Acknowledgements

665 We are grateful to the captain, crew members and scientific party of the R/V *Xuelong* for their help with the retrieval of the surface water suspended particulate matter and surface sediments. We also thank Fanny Kaczmar who helped produce HBI data at LOCEAN and to Dr. Guillaume Massé for supplying chemical standards for HBI quantification. We thank the Centre National de la Recherche Scientifique (CNRS) for salary support of M.-A.S. and V. K.

670 and for biomarker analyses. We thank Zhongqiang Ji, Liang Su and Yang Zhang for TOC and TN determinations of surface sediments, Dr. Hongliang Li and Yanpei Zhuang for sediment sampling and Qiang Hao for Chl *a* analyses in the surface water. We also thank Dr. Xiaotong Xiao and Dr. Long Lin for assistance in retrieving sea-ice concentration data. The pigments data used in this work are available in the Data-sharing Platform of Polar Science

675 (https://datacenter.chinare.org.cn/) maintained by the Chinese National Arctic & Antarctic Data Center (CN-NADC).

Financial support

This study was funded by the National Key Research and Development Program of China

680 (Nos. 2019YFE0120900), the National Natural Science Foundation of China (Nos. 41976229, 41941013, 41776205, 42076241 and 42376243), the Scientific Research Funds of the Second Institute of Oceanography, MNR (No. JG2310), the Chinese Polar Environmental

Comprehensive Investigation and Assessment Programs (No. CHINARE 0304), and the project ICAR (Sea Ice melt, Carbon, Acidification and Phytoplankton in the present and past Arctic Ocean) funded by Cai Yuan Pei Program.

685

References

Ardyna, M. and Arrigo, K. R.: Phytoplankton dynamics in a changing Arctic Ocean, Nature Climate Change, 10, 892-903, 10.1038/s41558-020-0905-y, 2020.

690 Ardyna, M., Babin, M., Gosselin, M., Devred, E., Rainville, L., and Tremblay, J.-É.: Recent Arctic Ocean sea ice loss triggers novel fall phytoplankton blooms, Geophysical Research Letters, 41, 6207-6212, https://doi.org/10.1002/2014GL061047, 2014.

Ardyna, M., Mundy, C. J., Mayot, N., Matthes, L. C., Oziel, L., Horvat, C., Leu, E., Assmy, P., Hill, V., Matrai, P. A., Gale, M., Melnikov, I. A., and Arrigo, K. R.: Under-Ice Phytoplankton Blooms: Shedding Light on the "Invisible" Part of Arctic Primary
695 Production, Frontiers in Marine Science, 7, 10.3389/fmars.2020.608032, 2020.

Arrigo, K. R. and van Dijken, G. L.: Secular trends in Arctic Ocean net primary production, Journal of Geophysical Research: Oceans, 116, https://doi.org/10.1029/2011JC007151, 2011.

Arrigo, K. R., Perovich, D. K., Pickart, R. S., Brown, Z. W., van Dijken, G. L., Lowry, K.
700 E., Mills, M. M., Palmer, M. A., Balch, W. M., Bahr, F., Bates, N. R., Benitez-Nelson, C., Bowler, B., Brownlee, E., Ehn, J. K., Frey, K. E., Garley, R., Laney, S. R., Lubelczyk, L., Mathis, J., Matsuoka, A., Mitchell, B. G., Moore, G. W. K., Ortega-Retuerta, E., Pal, S., Polashenski, C. M., Reynolds, R. A., Schieber, B., Sosik, H. M., Stephens, M., and Swift, J. H.: Massive Phytoplankton Blooms Under Arctic Sea Ice,
705 Science, 336, 1408-1408, doi:10.1126/science.1215065, 2012.

Arrigo, K. R.: Sea ice as a habitat for primary producers, in: Sea Ice, 352-369, https://doi.org/10.1002/9781118778371.ch14, 2017.

Bai, Y., Sicre, M.-A., Chen, J., Klein, V., Jin, H., Ren, J., Li, H., Xue, B., Ji, Z., Zhuang, Y., and Zhao, M.: Seasonal and spatial variability of sea ice and phytoplankton
710 biomarker flux in the Chukchi sea (western Arctic Ocean), Progress in Oceanography, 171, 22-37, https://doi.org/10.1016/j.pocean.2018.12.002, 2019.

Belt, S. T. and Müller, J.: The Arctic sea ice biomarker IP25: a review of current understanding, recommendations for future research and applications in palaeo sea ice reconstructions, Quaternary Science Reviews, 79, 9-25,
715 https://doi.org/10.1016/j.quascirev.2012.12.001, 2013.

Belt, S. T., Brown, T. A., Smik, L., Tatarek, A., Wiktor, J., Stowasser, G., Assmy, P., Allen, C. S., and Husum, K.: Identification of C25 highly branched isoprenoid (HBI) alkenes in diatoms of the genus Rhizosolenia in polar and sub-polar marine phytoplankton, Organic Geochemistry, 110, 65-72, https://doi.org/10.1016/j.orggeochem.2017.05.007,
720 2017.

Belt, S. T., Cabedo-Sanz, P., Smik, L., Navarro-Rodriguez, A., Berben, S. M. P., Knies, J., and Husum, K.: Identification of paleo Arctic winter sea ice limits and the marginal ice zone: Optimised biomarker-based reconstructions of late Quaternary Arctic sea ice, Earth and Planetary Science Letters, 431, 127-139,
725 https://doi.org/10.1016/j.epsl.2015.09.020, 2015.

Belt, S. T., Massé, G., Rowland, S. J., Poulin, M., Michel, C., and LeBlanc, B.: A novel chemical fossil of palaeo sea ice: IP25, Organic Geochemistry, 38, 16-27, https://doi.org/10.1016/j.orggeochem.2006.09.013, 2007.

Belt, S. T.: Source-specific biomarkers as proxies for Arctic and Antarctic sea ice, Organic
730 Geochemistry, 125, 277-298, https://doi.org/10.1016/j.orggeochem.2018.10.002, 2018.

Boetius, A., Albrecht, S., Bakker, K., Bienhold, C., Felden, J., Fernández-Méndez, M., Hendricks, S., Katlein, C., Lalande, C., Krumpen, T., Nicolaus, M., Peeken, I., Rabe, B., Rogacheva, A., Rybakova, E., Somavilla, R., Wenzhöfer, F., and Party, R. P. A.-.- S. S.: Export of Algal Biomass from the Melting Arctic Sea Ice, Science, 339, 1430-
735 1432, doi:10.1126/science.1231346, 2013.

Brabets, T.P., Wang, B., Meade, R.H.: Environmental and hydrologic overview of the Yukon River Basin, Alaska and Canada, U.S. Geological Survey Water-Resources Investigations Report, 99-4204 (106 pp.), 2000.

Brown, K. A., Holding, J. M., and Carmack, E. C.: Understanding Regional and Seasonal Variability Is Key to Gaining a Pan-Arctic Perspective on Arctic Ocean Freshening, Frontiers in Marine Science, 7, 10.3389/fmars.2020.00606, 2020.

Brown, T. A., Belt, S. T., Philippe, B., Mundy, C. J., Massé, G., Poulin, M., and Gosselin, M.: Temporal and vertical variations of lipid biomarkers during a bottom ice diatom bloom in the Canadian Beaufort Sea: further evidence for the use of the IP25 biomarker as a proxy for spring Arctic sea ice, Polar Biology, 34, 1857-1868, 10.1007/s00300-010-0942-5, 2011.

Brown, T. A., Belt, S. T., Tatarek, A., and Mundy, C. J.: Source identification of the Arctic sea ice proxy IP25, Nature communications, 5, 4197, 10.1038/ncomms5197, 2014a.

Brown, T. A., Yurkowski, D. J., Ferguson, S. H., Alexander, C., and Belt, S. T.: H-Print: a new chemical fingerprinting approach for distinguishing primary production sources in Arctic ecosystems, Environmental Chemistry Letters, 12, 387-392, 10.1007/s10311-014-0459-1, 2014b.

Cautain, I. J., Last, K. S., McKee, D., Bluhm, B. A., Renaud, P. E., Ziegler, A. F., and Narayanaswamy, B. E.: Uptake of sympagic organic carbon by the Barents Sea benthos linked to sea ice seasonality, Frontiers in Marine Science, 9, 10.3389/fmars.2022.1009303, 2022.

Coachman, L. K., Aagaard, K., and Tripp, R. B.: Bering Strait: the regional physical oceanography, University of Washington Press,1975.

Coupel, P., Jin, H. Y., Joo, M., Horner, R., Bouvet, H. A., Sicre, M. A., Gascard, J. C., Chen, J. F., Garçon, V., and Ruiz-Pino, D.: Phytoplankton distribution in unusually low sea ice cover over the Pacific Arctic, Biogeosciences, 9, 4835-4850, 10.5194/bg-9-4835-2012, 2012.

Coupel, P., Ruiz-Pino, D., Sicre, M. A., Chen, J. F., Lee, S. H., Schiffrine, N., Li, H. L., and Gascard, J. C.: The impact of freshening on phytoplankton production in the Pacific Arctic Ocean, Progress in Oceanography, 131, 113-125, https://doi.org/10.1016/j.pocean.2014.12.003, 2015.

Darby, D. A., Ortiz, J., Polyak, L., Lund, S., Jakobsson, M., and Woodgate, R. A.: The role of currents and sea ice in both slowly deposited central Arctic and rapidly deposited Chukchi–Alaskan margin sediments, Global and Planetary Change, 68, 58-72, https://doi.org/10.1016/j.gloplacha.2009.02.007, 2009.

DiGirolamo, N. E., Parkinson, C. L., Cavalieri, D. J., Gloersen, P., and Zwally, H. J.: Sea Ice Concentrations from Nimbus-7 SMMR and DMSP SSM/I-SSMIS Passive Microwave Data, Version 2 [Data Set]. Boulder, Colorado USA. NASA National Snow and Ice Data Center Distributed Active Archive Center. https://doi.org/10.5067/MPYG15WAA4WX, 2022. [Date Accessed 11-14-2023].

Ehrlich, J., Bluhm, B. A., Peeken, I., Massicotte, P., Schaafsma, F. L., Castellani, G., Brandt, A., and Flores, H.: Sea-ice associated carbon flux in Arctic spring, Elementa: Science of the Anthropocene, 9, 10.1525/elementa.2020.00169, 2021.

Eicken, H., Gradinger, R., Gaylord, A., Mahoney, A., Rigor, I., and Melling, H.: Sediment transport by sea ice in the Chukchi and Beaufort Seas: Increasing importance due to changing ice conditions?, Deep Sea Research Part II: Topical Studies in Oceanography, 52, 3281-3302, 2005.

Fahl, K. and Stein, R.: Biomarkers as organic-carbon-source and environmental indicators in the Late Quaternary Arctic Ocean: problems and perspectives, Marine Chemistry, 63, 293-309, https://doi.org/10.1016/S0304-4203(98)00068-1, 1999.

Fernández-Méndez, M., Katlein, C., Rabe, B., Nicolaus, M., Peeken, I., Bakker, K., Flores, H., and Boetius, A.: Photosynthetic production in the central Arctic Ocean during the record sea-ice minimum in 2012, Biogeosciences, 12, 3525-3549, 10.5194/bg-12-3525-2015, 2015.

790 Gal, J.-K., Ha, S.-Y., Park, J., Shin, K.-H., Kim, D., Kim, N.-Y., Kang, S.-H., and Yang, E. J.: Seasonal Flux of Ice-Related Organic Matter During Under-Ice Blooms in the Western Arctic Ocean Revealed by Algal Lipid Biomarkers, Journal of Geophysical Research: Oceans, 127, e2021JC017914, https://doi.org/10.1029/2021JC017914, 2022.

Gosselin, M., Levasseur, M., Wheeler, P. A., Horner, R. A., and Booth, B. C.: New
795 measurements of phytoplankton and ice algal production in the Arctic Ocean, Deep Sea Research Part II: Topical Studies in Oceanography, 44, 1623-1644, https://doi.org/10.1016/S0967-0645(97)00054-4, 1997.

Gradinger, R.: Sea-ice algae: Major contributors to primary production and algal biomass in the Chukchi and Beaufort Seas during May/June 2002, Deep Sea Research Part II:
800 Topical Studies in Oceanography, 56, 1201-1212, https://doi.org/10.1016/j.dsr2.2008.10.016, 2009.

Gradinger, R.: Vertical fine structure of the biomass and composition of algal communities in Arctic pack ice, Marine Biology, 133, 745-754, 10.1007/s002270050516, 1999.

Grebmeier, J. M., Cooper, L. W., Feder, H. M., and Sirenko, B. I.: Ecosystem dynamics of
805 the Pacific-influenced Northern Bering and Chukchi Seas in the Amerasian Arctic, Progress in Oceanography, 71, 331-361, https://doi.org/10.1016/j.pocean.2006.10.001, 2006.

Grebmeier, J. M., McRoy, C. P., and Feder, H. M.: Pelagic-benthic coupling on the shelf of the northern Bering and Chukchi Seas. I. Food supply source and benthic biomass,
810 Marine Ecology Progress Series, 48, 57-67, 1988.

Grice, K., Klein Breteler, W. C. M., Schouten, S., Grossi, V., de Leeuw, J. W., and Damsté, J. S. S.: Effects of zooplankton herbivory on biomarker proxy records, Paleoceanography, 13, 686-693, https://doi.org/10.1029/98PA01871, 1998.

Harada, N.: Review: Potential catastrophic reduction of sea ice in the western Arctic Ocean:
815 Its impact on biogeochemical cycles and marine ecosystems, Global and Planetary Change, 136, 1-17, https://doi.org/10.1016/j.gloplacha.2015.11.005, 2016.

Harper, J. R.: Coastal Erosion Rates along the Chukchi Sea Coast Near Barrow, Alaska, Arctic, 31, 428-433, 1978.

Hill, V., Ardyna, M., Lee, S. H., and Varela, D. E.: Decadal trends in phytoplankton
820 production in the Pacific Arctic Region from 1950 to 2012, Deep Sea Research Part II: Topical Studies in Oceanography, 152, 82-94, https://doi.org/10.1016/j.dsr2.2016.12.015, 2018.

Holm-Hansen, O., Lorenzen, C. J., Holmes, R. W., and Strickland, J. D. H.: Fluorometric Determination of Chlorophyll, ICES Journal of Marine Science, 30, 3-15,
825 10.1093/icesjms/30.1.3, 1965.

Hop, H., Vihtakari, M., Bluhm, B. A., Assmy, P., Poulin, M., Gradinger, R., Peeken, I., von Quillfeldt, C., Olsen, L. M., Zhitina, L., and Melnikov, I. A.: Changes in Sea-Ice Protist Diversity With Declining Sea Ice in the Arctic Ocean From the 1980s to 2010s, Frontiers in Marine Science, 7, 10.3389/fmars.2020.00243, 2020.

830 Hunt Jr, G. L., Stabeno, P., Walters, G., Sinclair, E., Brodeur, R. D., Napp, J. M., and Bond, N. A.: Climate change and control of the southeastern Bering Sea pelagic ecosystem, Deep Sea Research Part II: Topical Studies in Oceanography, 49, 5821-5853, https://doi.org/10.1016/S0967-0645(02)00321-1, 2002.

Hunt, G. L., Blanchard, A. L., Boveng, P., Dalpadado, P., Drinkwater, K. F., Eisner, L.,
835 Hopcroft, R. R., Kovacs, K. M., Norcross, B. L., Renaud, P., Reigstad, M., Renner, M., Skjoldal, H. R., Whitehouse, A., and Woodgate, R. A.: The Barents and Chukchi Seas:

Comparison of two Arctic shelf ecosystems, Journal of Marine Systems, 109-110, 43-68, https://doi.org/10.1016/j.jmarsys.2012.08.003, 2013.

840   Huntington, H. P., Danielson, S. L., Wiese, F. K., Baker, M., Boveng, P., Citta, J. J., De Robertis, A., Dickson, D. M. S., Farley, E., George, J. C., Iken, K., Kimmel, D. G., Kuletz, K., Ladd, C., Levine, R., Quakenbush, L., Stabeno, P., Stafford, K. M., Stockwell, D., and Wilson, C.: Evidence suggests potential transformation of the Pacific Arctic ecosystem is underway, Nature Climate Change, 10, 342-348, 10.1038/s41558-020-0695-2, 2020.

845   IPCC. In Masson-Delmotte, V., Zhai, P., Pirani, A., Connors, S. L., Péan, C., Berger, S., Caud, N., Chen, Y., Goldfarb, L., Gomis, M. I., Huang, M., Leitzell, K., Lonnoy, E., Matthews, J. B. R., Maycock, T. K., Waterfield, T., Yelekçi, O., Yu, R., & Zhou B., (Eds.) Climate change 2021: The physical science basis. Contribution of Working Group I to the Sixth assessment report of the intergovernmental panel on climate
850   change. Cambridge University Press.

Jakobsson, M., Andreassen, K., Bjarnadóttir, L. R., Dove, D., Dowdeswell, J. A., England, J. H., Funder, S., Hogan, K., Ingólfsson, Ó., Jennings, A., Krog Larsen, N., Kirchner, N., Landvik, J. Y., Mayer, L., Mikkelsen, N., Möller, P., Niessen, F., Nilsson, J., O'Regan, M., Polyak, L., Nørgaard-Pedersen, N., and Stein, R.: Arctic Ocean glacial
855   history, Quaternary Science Reviews, 92, 40-67, https://doi.org/10.1016/j.quascirev.2013.07.033, 2014.

Ji, R., Ashjian, C. J., Campbell, R. G., Chen, C., Gao, G., Davis, C. S., Cowles, G. W., and Beardsley, R. C.: Life history and biogeography of Calanus copepods in the Arctic Ocean: An individual-based modeling study, Progress in Oceanography, 96, 40-56,
860   https://doi.org/10.1016/j.pocean.2011.10.001, 2012.

Ji, Z., Jin, H., Stein, R., Li, Z., Bai, Y., Li, H., Zhang, Y., and Chen, J.: Distribution and Sources of Organic Matter in Surface Sediments of the Northern Bering and Chukchi Seas by Using Bulk and Tetraether Proxies, Journal of Ocean University of China, 18, 563-572, 10.1007/s11802-019-3869-7, 2019.

865   Jin, M., Deal, C., Lee, S. H., Elliott, S., Hunke, E., Maltrud, M., and Jeffery, N.: Investigation of Arctic sea ice and ocean primary production for the period 1992–2007 using a 3-D global ice–ocean ecosystem model, Deep Sea Research Part II: Topical Studies in Oceanography, 81-84, 28-35, https://doi.org/10.1016/j.dsr2.2011.06.003, 2012.

870   Kahru, M., Lee, Z., Mitchell, B. G., and Nevison, C. D.: Effects of sea ice cover on satellite-detected primary production in the Arctic Ocean, Biology Letters, 12, 20160223, doi:10.1098/rsbl.2016.0223, 2016.

Koch, C. W., Cooper, L. W., Lalande, C., Brown, T. A., Frey, K. E., and Grebmeier, J. M.: Seasonal and latitudinal variations in sea ice algae deposition in the Northern Bering
875   and Chukchi Seas determined by algal biomarkers, PLOS ONE, 15, e0231178, 10.1371/journal.pone.0231178, 2020a.

Koch, C. W., Cooper, L. W., Grebmeier, J. M., Frey, K., and Brown, T. A.: Ice algae resource utilization by benthic macro-and megafaunal communities on the Pacific Arctic shelf determined through lipid biomarker analysis, Marine Ecology Progress
880   Series, 651, 23-43, 2020b.

Koch, C. W., Brown, T. A., Amiraux, R., Ruiz-Gonzalez, C., MacCorquodale, M., Yunda-Guarin, G. A., Kohlbach, D., Loseto, L. L., Rosenberg, B., and Hussey, N. E.: Year-round utilization of sea ice-associated carbon in Arctic ecosystems, Nature communications, 14, 1964, 2023.

885   Kohlbach, D., Graeve, M., A. Lange, B., David, C., Peeken, I., and Flores, H.: The importance of ice algae-produced carbon in the central Arctic Ocean ecosystem: Food

web relationships revealed by lipid and stable isotope analyses, Limnology and Oceanography, 61, 2027-2044, https://doi.org/10.1002/lno.10351, 2016.

Kolling, H. M., Stein, R., Fahl, K., Sadatzki, H., de Vernal, A., and Xiao, X.: Biomarker Distributions in (Sub)-Arctic Surface Sediments and Their Potential for Sea Ice Reconstructions, Geochemistry, Geophysics, Geosystems, 21, e2019GC008629, https://doi.org/10.1029/2019GC008629, 2020.

Kolling, H., Schneider, R., Gross, F., Hamann, C., Kienast, M., Kienast, S., Doering, K., Fahl, K., and Stein, R.: Biomarker Records of Environmental Shifts on the Labrador Shelf During the Holocene, Paleoceanography and Paleoclimatology, 38, e2022PA004578, https://doi.org/10.1029/2022PA004578, 2023.

Lannuzel, D., Tedesco, L., van Leeuwe, M., Campbell, K., Flores, H., Delille, B., Miller, L., Stefels, J., Assmy, P., Bowman, J., Brown, K., Castellani, G., Chierici, M., Crabeck, O., Damm, E., Else, B., Fransson, A., Fripiat, F., Geilfus, N.-X., Jacques, C., Jones, E., Kaartokallio, H., Kotovitch, M., Meiners, K., Moreau, S., Nomura, D., Peeken, I., Rintala, J.-M., Steiner, N., Tison, J.-L., Vancoppenolle, M., Van der Linden, F., Vichi, M., and Wongpan, P.: The future of Arctic sea-ice biogeochemistry and ice-associated ecosystems, Nature Climate Change, 10, 983-992, 10.1038/s41558-020-00940-4, 2020.

Legendre, L., Ackley, S. F., Dieckmann, G. S., Gulliksen, B., Horner, R., Hoshiai, T., Melnikov, I. A., Reeburgh, W. S., Spindler, M., and Sullivan, C. W.: Ecology of sea ice biota, Polar Biology, 12, 429-444, 10.1007/BF00243114, 1992.

Leu, E., Søreide, J. E., Hessen, D. O., Falk-Petersen, S., and Berge, J.: Consequences of changing sea-ice cover for primary and secondary producers in the European Arctic shelf seas: Timing, quantity, and quality, Progress in Oceanography, 90, 18-32, https://doi.org/10.1016/j.pocean.2011.02.004, 2011.

Li, W. K., McLaughlin, F. A., Lovejoy, C., and Carmack, E. C.: Smallest algae thrive as the Arctic Ocean freshens, Science, 326, 539-539, 2009.

Massé, G., Rowland, S. J., Sicre, M.-A., Jacob, J., Jansen, E., and Belt, S. T.: Abrupt climate changes for Iceland during the last millennium: Evidence from high resolution sea ice reconstructions, Earth and Planetary Science Letters, 269, 565-569, https://doi.org/10.1016/j.epsl.2008.03.017, 2008.

Méheust, M., Fahl, K., and Stein, R.: Variability in modern sea surface temperature, sea ice and terrigenous input in the sub-polar North Pacific and Bering Sea: Reconstruction from biomarker data, Organic Geochemistry, 57, 54-64, https://doi.org/10.1016/j.orggeochem.2013.01.008, 2013.

Moore, S. E. and Grebmeier, J. M.: The Distributed Biological Observatory:Linking Physics to Biology in the Pacific Arctic Region, Arctic, 71, 1-7, 2018.

Moran, S. B., Lomas, M. W., Kelly, R. P., Gradinger, R., Iken, K., and Mathis, J. T.: Seasonal succession of net primary productivity, particulate organic carbon export, and autotrophic community composition in the eastern Bering Sea, Deep Sea Research Part II: Topical Studies in Oceanography, 65-70, 84-97, https://doi.org/10.1016/j.dsr2.2012.02.011, 2012.

Müller, J., Wagner, A., Fahl, K., Stein, R., Prange, M., and Lohmann, G.: Towards quantitative sea ice reconstructions in the northern North Atlantic: A combined biomarker and numerical modelling approach, Earth and Planetary Science Letters, 306, 137-148, 10.1016/j.epsl.2011.04.011, 2011.

Naidu, A., Cooper, L., Grebmeier, J., Whitledge, T., and Hameedi, M.: The continental margin of the North Bering-Chukchi Sea: concentrations, sources, fluxes, accumulation and burial rates of organic carbon, The Organic Carbon Cycle in the Arctic Ocean, 193-203, 2004.

Park, Y.-H., Yamamoto, M., Nam, S.-I., Irino, T., Polyak, L., Harada, N., Nagashima, K., Khim, B.-K., Chikita, K., and Saitoh, S.-I.: Distribution, source and transportation of

glycerol dialkyl glycerol tetraethers in surface sediments from the western Arctic Ocean and the northern Bering Sea, Marine Chemistry, 165, 10-24, https://doi.org/10.1016/j.marchem.2014.07.001, 2014.

940

Park, J. H., Kim, S.-J., Lim, H.-G., Kug, J.-S., Yang, E. J., and Kim, B.-M.: Phytoplankton responses to increasing Arctic river discharge under the present and future climate simulations, Environmental Research Letters, 18, 064037, 10.1088/1748-9326/acd568, 2023.

945

Pearce, C., Varhelyi, A., Wastegård, S., Muschitiello, F., Barrientos, N., O'Regan, M., Cronin, T. M., Gemery, L., Semiletov, I., Backman, J., and Jakobsson, M.: The 3.6 ka Aniakchak tephra in the Arctic Ocean: a constraint on the Holocene radiocarbon reservoir age in the Chukchi Sea, Clim. Past, 13, 303-316, 10.5194/cp-13-303-2017, 2017.

950

Pickart, R. S., Spall, M. A., Moore, G. W. K., Weingartner, T. J., Woodgate, R. A., Aagaard, K., and Shimada, K.: Upwelling in the Alaskan Beaufort Sea: Atmospheric forcing and local versus non-local response, Progress in Oceanography, 88, 78-100, https://doi.org/10.1016/j.pocean.2010.11.005, 2011.

Polyak, L., Bischof, J., Ortiz, J. D., Darby, D. A., Channell, J. E. T., Xuan, C., Kaufman, D. S., Løvlie, R., Schneider, D. A., Eberl, D. D., Adler, R. E., and Council, E. A.: Late Quaternary stratigraphy and sedimentation patterns in the western Arctic Ocean, Global and Planetary Change, 68, 5-17, https://doi.org/10.1016/j.gloplacha.2009.03.014, 2009.

955

Renaut, S., Devred, E., and Babin, M.: Northward Expansion and Intensification of Phytoplankton Growth During the Early Ice-Free Season in Arctic, Geophysical Research Letters, 45, 10,590-510,598, https://doi.org/10.1029/2018GL078995, 2018.

960

Roach, A. T., Aagaard, K., Pease, C. H., Salo, S. A., Weingartner, T., Pavlov, V., and Kulakov, M.: Direct measurements of transport and water properties through the Bering Strait, Journal of Geophysical Research: Oceans, 100, 18443-18457, https://doi.org/10.1029/95JC01673, 1995.

965

Schlitzer, Reiner, Ocean Data View, odv.awi.de, 2023.

Schmidt, K., Brown, T. A., Belt, S. T., Ireland, L. C., Taylor, K. W. R., Thorpe, S. E., Ward, P., and Atkinson, A.: Do pelagic grazers benefit from sea ice? Insights from the Antarctic sea ice proxy IPSO25, Biogeosciences, 15, 1987-2006, 10.5194/bg-15-1987-2018, 2018.

970

Shimada, K., Kamoshida, T., Itoh, M., Nishino, S., Carmack, E., McLaughlin, F., Zimmermann, S., and Proshutinsky, A.: Pacific Ocean inflow: Influence on catastrophic reduction of sea ice cover in the Arctic Ocean, Geophysical Research Letters, 33, https://doi.org/10.1029/2005GL025624, 2006.

Smik, L., Cabedo-Sanz, P., and Belt, S. T.: Semi-quantitative estimates of paleo Arctic sea ice concentration based on source-specific highly branched isoprenoid alkenes: A further development of the PIP25 index, Organic Geochemistry, 92, 63-69, https://doi.org/10.1016/j.orggeochem.2015.12.007, 2016.

975

Søreide,, J. E., Leu, E., Berge, J., Graeve, M., and Falk-Petersen, S.: Timing of blooms, algal food quality and Calanus glacialis reproduction and growth in a changing Arctic, Global Change Biology, 16, 3154-3163, https://doi.org/10.1111/j.1365-2486.2010.02175.x, 2010.

980

Stabeno, P. J. and Reed, R. K.: Circulation in the Bering Sea Basin Observed by Satellite-Tracked Drifters: 1986–1993, Journal of Physical Oceanography, 24, 848-854, https://doi.org/10.1175/1520-0485(1994)024<0848:CITBSB>2.0.CO;2, 1994.

985

Stein, R., Matthiessen, J., Niessen, F., Krylov, A., Nam, S.-i., and Bazhenova, E.: Towards a better (litho-) stratigraphy and reconstruction of Quaternary paleoenvironment in the Amerasian Basin (Arctic Ocean), Polarforschung, 79, 97-121, 2010.

990 Stein, R., Fahl, K., Schreck, M., Knorr, G., Niessen, F., Forwick, M., Gebhardt, C., Jensen, L., Kaminski, M., and Kopf, A.: Evidence for ice-free summers in the late Miocene central Arctic Ocean, Nature communications, 7, 11148, 2016.

Su, L., Ren, J., Sicre, M. A., Bai, Y., Zhao, R., Han, X., Li, Z., Jin, H., Astakhov, A. S., Shi, X., and Chen, J.: Changing sources and burial of organic carbon in the Chukchi Sea sediments with retreating sea ice over recent centuries, Clim. Past, 19, 1305-1320, 10.5194/cp-19-1305-2023, 2023.

995 Su, L., Ren, J., Sicre, M.-A., Bai, Y., Jalali, B., Li, Z., Jin, H., Astakhov, A. S., Shi, X., and Chen, J.: HBIs and Sterols in Surface Sediments Across the East Siberian Sea: Implications for Palaeo Sea-Ice Reconstructions, Geochemistry, Geophysics, Geosystems, 23, e2021GC009940, https://doi.org/10.1029/2021GC009940, 2022.

Tedesco, L., Vichi, M., and Scoccimarro, E.: Sea-ice algal phenology in a warmer Arctic, 1000 Science Advances, 5, eaav4830, doi:10.1126/sciadv.aav4830, 2019.

Tolosa, I., Fiorini, S., Gasser, B., Martín, J., and Miquel, J. C.: Carbon sources in suspended particles and surface sediments from the Beaufort Sea revealed by molecular lipid biomarkers and compound-specific isotope analysis, Biogeosciences, 10, 2061-2087, 10.5194/bg-10-2061-2013, 2013.

1005 Volkman, J. K.: A review of sterol markers for marine and terrigenous organic matter, Organic Geochemistry, 9, 83-99, https://doi.org/10.1016/0146-6380(86)90089-6, 1986.

Volkman, J.K.: Sterols in Microalgae. In: Borowitzka, M.A., Beardall, J., Raven, J.A. (Eds.), The Physiology of Microalgae. Springer International Publishing, Cham, pp. 485–505, 2016.

1010 Walsh, J. E., Fetterer, F., Scott stewart, J., and Chapman, W. L.: A database for depicting Arctic sea ice variations back to 1850, Geographical Review, 107, 89-107, 10.1111/j.1931-0846.2016.12195.x, 2017.

Weingartner, T. J., Danielson, S., Sasaki, Y., Pavlov, V., and Kulakov, M.: The Siberian Coastal Current: A wind- and buoyancy-forced Arctic coastal current, Journal of 1015 Geophysical Research: Oceans, 104, 29697-29713, https://doi.org/10.1029/1999JC900161, 1999.

Weingartner, T., Aagaard, K., Woodgate, R., Danielson, S., Sasaki, Y., and Cavalieri, D.: Circulation on the north central Chukchi Sea shelf, Deep Sea Research Part II: Topical Studies in Oceanography, 52, 3150-3174, https://doi.org/10.1016/j.dsr2.2005.10.015, 1020 2005.

Welschmeyer, N. A.: Fluorometric analysis of chlorophyll a in the presence of chlorophyll b and pheopigments, Limnology and Oceanography, 39, 1985-1992, https://doi.org/10.4319/lo.1994.39.8.1985, 1994.

Williford, K. H., Ward, P. D., Garrison, G. H., and Buick, R.: An extended organic carbon-1025 isotope record across the Triassic–Jurassic boundary in the Queen Charlotte Islands, British Columbia, Canada, Palaeogeography, Palaeoclimatology, Palaeoecology, 244, 290-296, https://doi.org/10.1016/j.palaeo.2006.06.032, 2007.

Woodgate, R. A., and Peralta-Ferriz, C.: Warming and Freshening of the Pacific Inflow to the Arctic From 1990-2019 Implying Dramatic Shoaling in Pacific Winter Water 1030 Ventilation of the Arctic Water Column, Geophysical Research Letters, 48, e2021GL092528, https://doi.org/10.1029/2021GL092528, 2021.

Woodgate, R. A. and Aagaard, K.: Revising the Bering Strait freshwater flux into the Arctic Ocean, Geophysical Research Letters, 32, https://doi.org/10.1029/2004GL021747, 2005.

1035 Woodgate, R. A., Aagaard, K., and Weingartner, T. J.: A year in the physical oceanography of the Chukchi Sea: Moored measurements from autumn 1990–1991, Deep Sea Research Part II: Topical Studies in Oceanography, 52, 3116-3149, https://doi.org/10.1016/j.dsr2.2005.10.016, 2005.

1040 Woodgate, R. A.: Increases in the Pacific inflow to the Arctic from 1990 to 2015, and insights into seasonal trends and driving mechanisms from year-round Bering Strait mooring data, Progress in Oceanography, 160, 124-154, https://doi.org/10.1016/j.pocean.2017.12.007, 2018.

Xiao, X., Fahl, K., Müller, J., and Stein, R.: Sea-ice distribution in the modern Arctic Ocean: Biomarker records from trans-Arctic Ocean surface sediments, Geochimica et Cosmochimica Acta, 155, 16-29, https://doi.org/10.1016/j.gca.2015.01.029, 2015.

1045

Yunker, M. B., Macdonald, R. W., Veltkamp, D. J., and Cretney, W. J.: Terrestrial and marine biomarkers in a seasonally ice-covered Arctic estuary — integration of multivariate and biomarker approaches, Marine Chemistry, 49, 1-50, https://doi.org/10.1016/0304-4203(94)00057-K, 1995.

1050 Zhuang, Y., Jin, H., Chen, J., Ren, J., Zhang, Y., Lan, M., Zhang, T., He, J., and Tian, J.: Phytoplankton Community Structure at Subsurface Chlorophyll Maxima on the Western Arctic Shelf: Patterns, Causes, and Ecological Importance, Journal of Geophysical Research: Biogeosciences, 125, e2019JG005570, https://doi.org/10.1029/2019JG005570, 2020.

1055